CHAPTER 5

Hill-Based Muscle Models: A Systems Engineering Perspective

Jack M. Winters

5.1 Introduction

Chapter 1 (Zahalak) provided a brief historical treatment of the early findings that led to the muscle model structure first proposed by A.V. Hill (1938). From a "systems engineering" perspective, this is a phenomenologically based, lumped-parameter model that is based on interpretations of input-output data obtained from controlled experiments. Simply stated, this model consists of a ***contractile element*** (*CE*) that is surrounded, both in series and in parallel, by "passive" connective tissue (Figure 5.1). *CE* is furthermore characterized by two fundamental relationships: *CE* tension–length and *CE* force–velocity. Each of these is modulated by an activation input that is structurally distinct from the location for mechanical coupling between the muscle and the environment (Figure 5.1).

This model has been (and remains) the model of choice for most modeling studies of multiple muscle movement systems. For example, it is explicitly utilized in Chapters 6–8, 10, 19, 21, 31, 38–39, and 41–43.

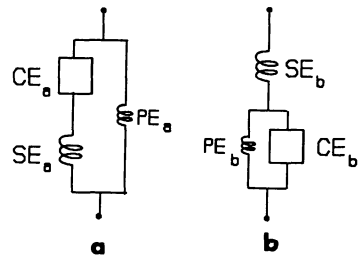

Figure 5.1: Classical structures for the Hill muscle model, with contractile element (*CE*), series element (*SE*, larger spring), parallel element (*PE*).

Part of the reason for the wide use of this model structure is that it describes most of the salient features of muscle mechanics quite well. A related reason is due to the ease with which model parameter values can be estimated; in fact, by my count over two dozen papers from over one dozen distinct groups have provided raw data explicitly in a form compatible with the Hill model structure.

However, as outlined in Chapter 1 (Zahalak), this model is far from perfect. Criticisms come from two extremes:

i) The model is ***too simple***, and fails to capture certain fundamental features of real muscle. Indeed, there have been suggestions, based on results from certain classes of controlled experiments on isolated fibers or a single muscle, that this model and its fundamental structure is inherently flawed and inadequate (Chapters 1–2). Consequently, it is suggested that it should be discarded in favor of more realistic (and complex) models.

ii) The model is ***overly complex***, with this complexity excessive for studies addressing underlying principles regarding multiple muscle movement organization. As such, it may limit one's vision. Rather, from this perspective muscle is viewed as either a force generator (e.g., based on interpretation of rectified and smoothed *EMG*s) or a spring (often with variable stiffness or rest length). This approach is used, either implicitly or explicitly, in Chapters 9, 12, 16–17, 24–27, 29–30, 32–33, 37, 40, 44–46).

Our primary goal in this chapter is to address these criticisms, with an emphasis on the first, which is a more serious charge. Such an assess-

Multiple Muscle Systems: Biomechanics and Movement Organization
J.M. Winters and S.L-Y. Woo (eds), © 1990 Springer-Verlag

ment of the strengths, weaknesses, and limitations of Hill-based models appears timely and especially appropriate within this book. Our secondary goal is to provide a reasonably deep foundation that will enable the novice to understand and effectively utilize (or reject!) this modeling foundation.

Our perspective will be that of a ***"systems engineer"*** interested in using a muscle model to help gain ***insight into dynamic movement systems that involve multiple muscles.*** We furthermore specify that adequate simulation only over a moderate operating range is unacceptable. More explicitly, we want to utilize a muscle model that we can ***trust***: while not perfect, each muscle modeled will ***never be far off*** for ***any*** musculoskeletal movement task of potential interest. Such a model would have a high capacity for providing insight and a negligible capacity for providing misinformation of significance.

In Section 5.2 we start with a brief historical introduction to the Hill-based model from a "systems" perspective, complimenting the review in Chapter 1 (Zahalak). Since the series and parallel elements within this model represent connective tissue, we then review the basic mechanical properties of such tissues. We then briefly distinguish between the structural forms of current Hill-based models. With the foundation established, in Section 5.3 we consider muscle properties, especially as related to constitutive relations for the basic components of the model.

In Section 5.4 we address experimental results that challenge the Hill model foundation. Our goal here is to: ***i)*** outline the nature of any discrepancies between experiment and Hill-model predictions; ***ii)*** see whether techniques exist for enhancing Hill-based so that these discrepancies are insignificant; and ***iii)*** assuming discrepancies still exist (or elimination comes at too high a computational or conceptual cost), discern whether or not these discrepancies are physiologically relevant for *in-situ* musculoskeletal systems. In Section 5.5 we outline some of the insights that are possible when utilizing Hill-based models that might be "missed" if muscle is simply assumed to be an idealized force generator or a simple spring, or if one is interpreting *EMG* data without the aid of a mathematical model. Finally, in Section 5.6 a few possible future directions are suggested.

5.2 Hill-Based "Systems" Muscle Model

5.2.1 Modeling Foundations

"Input–Output" Experiments

The conceptual foundation behind the early experimental investigations of Hill, Fenn, Wilkie, and colleagues have their root in what would now be called "systems physiology" or "systems engineering": controlled "black box" systems identification with fairly well-defined inputs and outputs, leading to models with a predictive capacity. This "systems" approach differs somewhat from the "reductionist" approach on which biophysical models of muscle are based (e.g., Chapters 1–2). (Although these two approaches often evolve somewhat independently, both are necessary.)

As seen in Figure 5.2, there are three potential "inputs" to a muscle: muscle load, muscle length, and muscle stimulation (secondary effects such as temperature or extracellular ionic balances are ignored here). The traditional experimental approach has been to specify the input sequence for neural stimulation and then ***either*** force or length/velocity; the other of the latter two becomes the measured output trajectory. Typically, one input is held constant while the other is varied as an impulse, step, ramp, sinusoid, or a "white noise" (random signal). Notice that many combinations are possible, and, as seen in Figure 5.2, many of the classic combinations have been given specific names.

The above input–output description is a simplification. As shown in Figure 5.2f, in practice the controlling/measuring apparatus that is coupled to the system may possess significant dynamics, which here could represent the mass of the measuring apparatus. Mechanically, there is inherently bidirectional energetic coupling between the muscle and its environment [see Chapter 7 (Hannaford and Winters) and Chapter 9 (Hogan)], and thus the "output" measure may be influenced by the confounding effects such as apparatus mass/inertia. Of note is that the early pioneers were very much aware of this influence and went to lengths to minimize such effects [e.g. the widely used two-lever scheme developed by Bouckaert et al. (1930)]. For human studies, efforts were made by Wilkie (1950) to mathematically subtract out the effects of inertia.

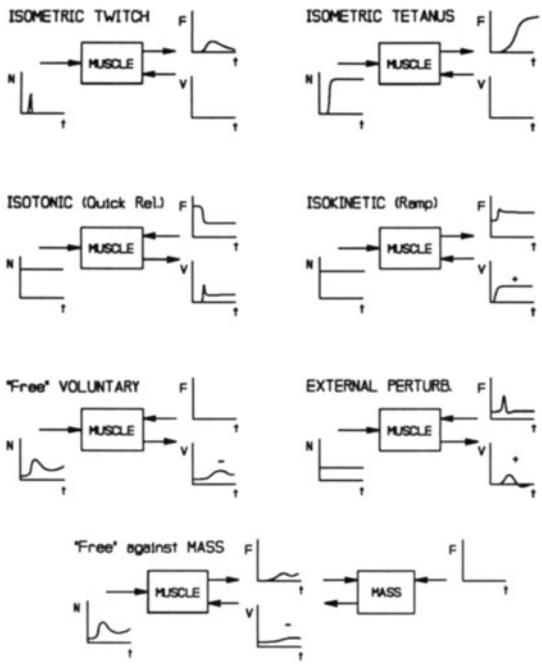

Figure 5.2: Input–output combinations for skeletal muscle. In each case the neural input (*N*) is on the left and the mechanical variable pair, force (*F*) and velocity (*v*), is on the right. Notice that in each case there are two input sequences and one output trajectory to be measured. An "impulse" is as an input of short time duration relative to the system response – the area under the curve determines the intensity. A "step" is a change in level that, relative to the overall system response, is rapid. A "ramp" is the derivative of a step.

5.2.2 Identification of Model Structure

Based on early experiments and observations on animal and human movements, primarily for contractions against inertial loads, Hill (1922) and Gasser and Hill (1924) viewed muscle as a spring-like structure working in a linearly viscous medium [see also Chapter 1 (Zahalak)]. Based on isokinetic experiments, Levin and Wyman (1927) proposed the developed a model consisting of a damped spring-like property in series with an undamped spring. Bouckaert et al. (1930) suggested that after the initial undamped change in length, the remaining shortening followed a logarithmic relation. Fenn and Marsh (1935), introducing the concept of afterloaded isotonic contraction as a technique for isolating the damped component from the undamped component, determined that the force-velocity property was nonlinear rather than linear as Hill had originally suggested.

It was within this context that Hill published his famous 1938 paper which formally identified a lightly damped elastic element in series with a nonlinear *CE*. Furthermore, for maximal activation, the generated contractile force was found to decrease nonlinearly as the shortening velocity increased. This *CE* force–velocity behavior could be described, for shortening muscle, by a hyperbolic equation (other forms given in Section 5.3.3):

$$(F + a)(v + b) = (F_{max} + a)\, b \qquad (5.1)$$

where F is muscle tensile force, v is muscle shortening velocity, F_{max} is the maximum (tetanic) isometric force, and a and b are constants. The dimensionless "shape" parameter $a_f = a/F_{max} = b/v_{max}$, which specifies the hyperbolic concavity (Figure 5.2a), was found to have a value of about 0.25, approximately independent of length (however, see also Section 5.2.3). It was anticipated early on that the b parameter would have higher values for fast muscle fibers (Katz, 1939)). Hill also showed how *CE* could shorten during isometric contraction because of *SE* extension.

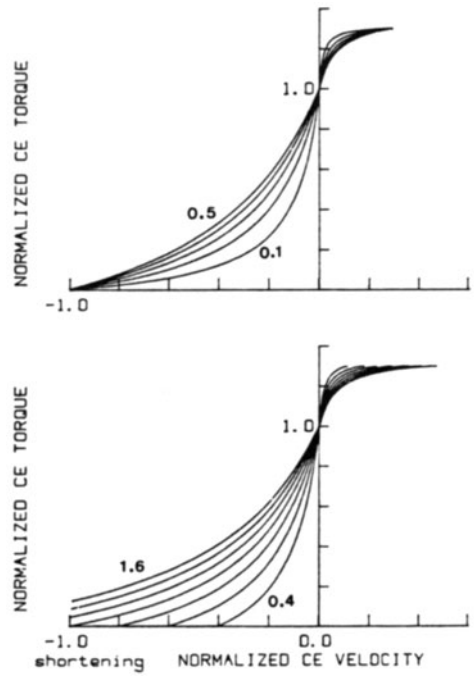

Figure 5.3: Effects of parameters on hyperbolic Hill equation (shortening to left). *a)* Variation in a_f. *b)* Variation in b (or v_{max} if a_f is assumed constant).

Katz (1939) showed that shortening contractions followed the Hill equation while lengthening contractions showed a greatly increased slope for lengthening muscle as opposed to shortening muscle and then exhibited significant "yielding," or "giving" (see also Chapters 1–3 and Section 5.4.1). This latter effect had been previously observed by others [e.g. Gasser and Hill (1924)] but not as succinctly described. Without the current insight into the molecular nature of the contractile machinery, as described in Chapters 1–4, explanations of this effect were clearly difficult.

In summary, the concept of a *CE* in ***series*** and in ***parallel*** (Figures 5–1a,b) with passive, lightly-damped elastic tissue was understood by 1939 [Katz (1939)]. However, since the parallel elasticity was typically small, it could effectively be ignored for most applications. This model structure, along with simplified versions of the activation process, can be considered as the foundation for the phenomenologically-based, lumped-parameter model of muscle. The concept behind the "active state" was in common use [e.g. "internal 'fundamental' mechanical change" in Gasser and Hill (1924), "active state" in Hill (1938)], but it was not until 1949 that Hill provided an explicit (albeit controversial) definition and a technique for estimating excitation–activation dynamics (see Section 5.3.4).

If the elements are linearized, Figures 5.1a and 5.1b can be shown to be equivalent. Defining the series and parallel springs as K_s and K_p, respectively, B as the internal Hill "viscosity" (see Figure 5.8), and F_o as the input to *CE*, the following relations hold between the elements of the two versions [e.g. McMahon (1984)]:

$$K_{s_b} = K_{s_a} + K_{p_a}; \qquad K_{p_a} = (K_{s_b} K_{p_b}) / K_{sp_b} \tag{5.2}$$

$$B_a / B_b = K_{s_a} / K_{sp_b}; \quad F_{o_a} / F_{o_b} = K_{s_b} / K_{sp_b}$$

where $K_{sp_b} = K_{s_b} + K_{p_b}$

5.2.3 Models for Soft Connective Tissues

Since *CE* is connected in series and parallel with viscoelastic tissues, it is appropriate to develop an understanding of the basic properties for such tissues. Passive soft connective tissues, ranging from tendon to skin to blood vessel, tend to have quasi-static mechanical properties such as shown in Figure 5.4a, in which the stiffness (slope of the curve) increase fairly linearly with force over the primary operating range [e.g. Fung (1967); Figure 5.4b]. This can be described mathematically:

$$\frac{dF}{dx} = K_1 F + K_2 \tag{5.3}$$

where F is force, x is extension, and K_i are constants (often $K_2 \approx 0$). Solving this equation and applying boundary conditions, we arrive at the classic exponential relationship for soft connective tissues (e.g., Fung, 1969; Hatze, 1974):

$$F = K_3 (e^{K_1 \Delta x} - 1) \tag{5.4}$$

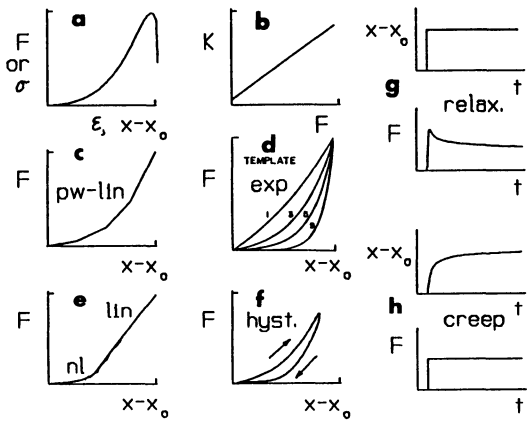

Figure 5.4: Classical mechanical properties of biological soft connective tissue. ***a)*** Typical quasi-static stress–strain or force–extension curves ($\sigma = F/$(cross-sectional area A); $\varepsilon = \Delta x/$(rest length L_o)). ***b)*** Classic stiffness–force relation, which results in the exponential force–extension behavior of *d)*. ***c)*** Concept of linear collagen fibers, of different initial orientation, starting to stretch at different extensions ("piecewise linear"). ***d)*** Exponential fit via "intuitive" parameters: a dimensionless "shape" parameter K_{sh} and a point on the curve (conveniently F_{max} and Δx_{max}). ***e)*** "Hybrid" curve: exponential "toe" segment followed by linear region. ***f)*** Hysteresis due to viscoelasticity for tissues under cyclic loading (constant velocity stretch followed by release). ***g)*** Force "relaxation" output trajectory due to a length step input. ***h)*** Length "creep" output trajectory due to a step change in force.

where Δx is the extension relative to the rest (i.e. zero force) length. For most tissues this behavior is due to wavy collagen fibers (which vary in number and orientation between tissues) gradually straightening out and bearing load (e.g., Fung, 1981). Thus, the overall curve could be exponentially shaped even if linear collagen properties are assumed (Figure 5.4c–d). This relation can be reformulated to possess a more convenient set of parameters (Hatze, 1981; Winters and Stark, 1985):

$$F_{se} = \left[\frac{F_1}{e^{K_{sh}} - 1} \right] \left(e^{(K_{sh}/\Delta x_1)\Delta x} - 1 \right) \quad (5.5)$$

where the describing parameters are now ***very intuitive***: a point on the curve (here F_1 and ε_1) and a dimensionless shape parameter (Figure 5.4d). In tendon and most ligaments most collagen fibers are initially orientated primarily along the long axis; this can result in flattening of the curve after the initial toe region (Woo et al., 1981). If desired, an exponentially-shaped toe region can easily be connected to a linear region, with the shape parameter set by the constraint of no discontinuity in slope (i.e. stiffness), as shown in Figure 5.4e.

Biological connective tissues are also inherently ***viscoelastic***, i.e., they exhibit hysteresis during cyclic loading (Figure 5.4f), force relaxation when held at a constant length (Figure 5.4g), and length creep when held at a constant force (Figure 5.4h). Of note is that viscoelastic effects are seen within both short (milliseconds) and long (minute or hours) time periods. Thus, the amount of hysteresis (measure of energy loss) varies with both the speed of ongoing extension and the history of recent extensions; hence a biomechanical basis for "stretching" before exercise.

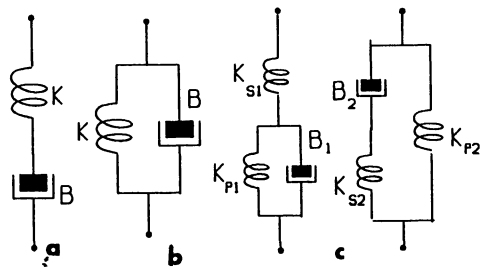

Figure 5.5: Classic models for describing viscoelastic properties. In each case the constitutive relation for the spring is $F = f(\Delta x)$, the dashpot is $F = f(\Delta v) = f(\Delta \dot{x})$. ***a)*** "Maxwell" series model. ***b)*** "Voigt" parallel model. ***c)*** "Kelvin," or "standard" models.

There are three classic models that have been used since the 1800's for describing basic viscoelastic behavior, with that of Figure 5.5c known to be more appropriate. (The "series" model of Figure 5.5a is inadequate during quasi-static conditions due to a tendency toward "drifting," while the "parallel" model of Figure 5.5b often poorly approximates initial transient behavior.) The series and parallel elements of the Hill model would be better represented by a Kelvin model; however, the added model complexity is usually considered not to be worth the burden. However, one must keep these ***passive properties in mind*** when ***interpreting*** muscle testing data, especially for experiments that unfold over ***very fast*** (order of milliseconds) or ***very slow*** (many seconds) time intervals. Interestingly, these are the time frames of most current muscle testing; hence the reason for considering passive properties in more depth than often seen in a "muscle mechanics" review. Over the moderate time range of most past musculotendon testing, long-term passive viscoelastic effects would appear as a slight drift.

5.2.4 Hill-Model Structural Extensions

Model structures for musculotendinous systems that have been commonly used are shown in Figure 5.1 and Figure 5.6. Essentially, the difference between these models is the arrangement of passive spring and dashpot elements. In both of these figures, springs with lower stiffness (higher compliance) are shown smaller. *Model d* is a better approximation of physical reality. However, is it worth the cost of the added complexity? If dashpots are assumed negligible (as is common), it turns out that some of the springs are ***not mathematically independent*** of each other. This can be seen by using methods such as *bond graphs* [see Chapter 7 (Hannaford and Winters)] to identify independent energy storage elements. When this is the case, models ***can be reduced*** without any loss to dynamic performance, and in fact, extra springs may confound interpretation and make modeling less computationally efficient. However, if an ***internal*** node location, such as *node d* in Figure 5.6, happens to be of special interest (e.g. for sensory feedback of muscle length), then the added structure is worthwhile. My own experience with various formulations is that the parallel elasticity is best lumped with joint properties [see Chapter 8 (Zajac and Winters)]. We will also see in Section 5.3.3 that the *CE* tension–length relation, although

"spring-like", is best not treated as a spring in parallel with a dashpot representing the *CE* force–velocity relation – the spring and dashpot forces would then be additive, which is ***not*** compatible with the *CE* force– velocity–length surface that is traditionally assumed to exist for each activation level. Upon reduction, we are back to an "equivalent" spring in series with a large *CE* "force-velocity" dashpot – the basic model structure which will serve as our base as we now develop each of the classic muscle properties.

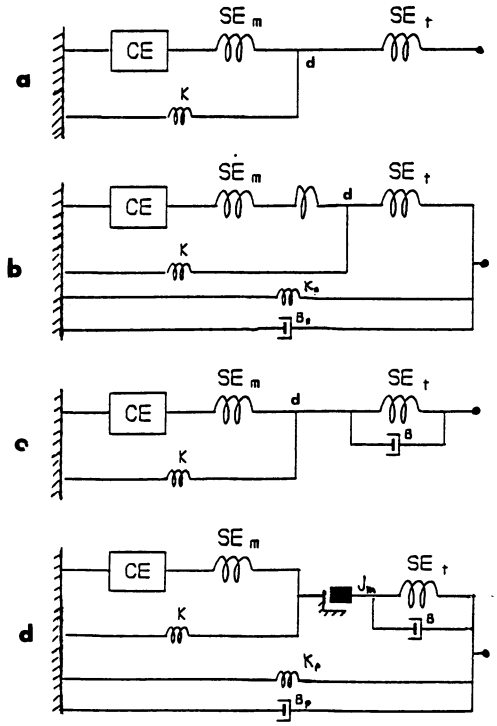

Figure 5.6: Common musculoskeletal model structures that go beyond those of Figure 5.1. ***a)*** Tendon in series with classic muscle structure. ***b)*** Combined muscle-tendon models with additional springs [see Hatze (1981) for details]. ***c)*** Simple model structure with a "lumped" *SE* viscoelastic element. ***d)*** "Complex" model which includes an internal node for muscle mass (the usual convention is to lump mass with the limb segment).

5.3 Model Parameter Identification

Since, mechanically, one can "see" the contractile machinery (for Hill-based models *CE*) only after connective tissue influence (even true for isolated muscle fibers), we start with *PE* and *SE* properties before considering *CE* properties.

5.3.1 Passive Parallel Element *(PE)*

This relation can be measured simply by pulling the passive muscle tissue at various specific (usually fairly slow) rates and measuring force. It is due primarily to the passive tissue within and surrounding muscle, and as with soft connective tissues in general, can be approximated by a viscoelastic model of one of the forms of Figure 5.5. The dashpot is typically neglected or assumed linear (Winters and Stark, 1985). For skeletal muscle the force developed by this element is insignificant except for extreme lengths (e.g over 1.2 times the rest length) which are often beyond the physiological range [e.g., Katz (1939, Bahler et al. (1967)]; hence its ***lack of inclusion*** within many models. For cardiac muscle, the parallel elasticity is significant [e.g., Parmley et al. (1970)]. For musculoskeletal systems the musculotendinous passive elements can be considered ***separately*** from the active muscle component, and lumped with other passive tissue in parallel if the passive element is considered to be a spring or a parallel arrangement of spring and dashpot and the model structure of Figure 5.1a is used [see also Section 8.3 of Chapter 8 (Zajac and Winters)]; this is the model structure that is recommended here.

5.3.2 Lightly Damped Series Element *(SE)*

Fundamental to the early work and all work since has been the concept of the lightly-damped elastic element is series with the contractile machinery. In fact it should be termed the series ***compliance*** element since the distinguishing feature is significant compliance, but in deference to history we will use the traditional terminology. Controversy surrounds the subtle details of this element [e.g. McMahon (1984)]; however, the fundamental existence of this type of property cannot be denied [Hill (1970)], and its use permeates this book (see especially Chapters 4, 34–37).

Three classic experimental techniques have been used to estimate this element [reviewed by Hill (1970)]: ***i)*** "controlled" stretch/release (Hill, 1950); ***ii)*** "quick release" (usually from tetanus [e.g., Wilkie, 1956)]; and ***iii)*** the isometric "calculation" method [Wilkie (1950)]. The second method has been most widely used. Some groups employing fast "controlled" stretch/releases have preferred terms such as "short-range" stiffness (Rack and Westbury, 1974) or "high frequency" stiffness (e.g., Cecchi et al., 1984) to distinguish the observed behavior from that of an ideally pas-

sive spring (the distinction is discussed later). In general, the results with the third method have predicted a more compliant relationship; reasons for this difference will become evident later. However, all techniques have produced concave upward load-extension curves, with peak element extensions between 2% and 8% [e.g., review by Close (1972)].

A fourth class of techniques involve consideration of muscle oscillation; authors' utilizing these methods have been hesitant to directly relate their "stiffness" findings to *SE*, but the estimated values is so compatible with those obtained from other techniques that it is hard to deny a correlation (e.g., see data of Zahalak and Heyman, 1979). When put together, there is remarkable consistency across the data, as will be seen below.

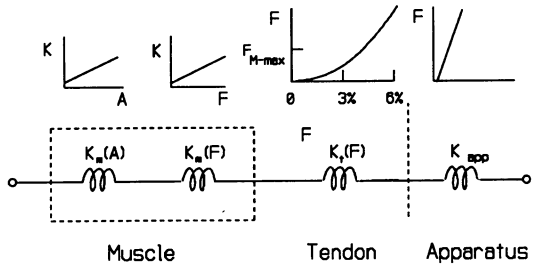

Figure 5.7: Conceptual model of four springs in series. *a)* The two left-most are within muscle tissue, with the stiffness (slope times initial length) potentially a function of both activation (far left, cross-bridges) and force (middle left, Z-discs and filaments). The stiffness for the middle-right curve, representing tendon, is a function of force, except perhaps at higher values. The right curve, representing the apparatus, is likely linear with potentially a slight offset due to stiction effects. *b)* Quasi-statically, the total curve is obtained by summing the individual extensions for each force level:

$$\delta L = (\delta L_{m_a} + \delta L_{m_p}) + \delta L_t + \delta L_a \qquad (5.6)$$

or:

$$= (L_{m_{o_a}} \varepsilon_m + L_{m_{o_p}} \varepsilon_m) + L_{t_o} \varepsilon_t + \delta L_a \qquad (5.7)$$

Thus, the relative extension due to each component is a function of the relative lengths. Also, because of the series arrangement, for a given force the individual compliances (inverse of stiffness) add; thus, the overall stiffness (compliance) is less than (more than) that of the individual components.

Overview of SE Structural Components. Figure 5.7 conceptually separates the "series element" into three components and an additional component for the apparatus. The complex aponeurosis structure (not shown) could perhaps be placed within the tendon, although as shown in Chapter 4 (Ettema and Huijing) this tissue has unique features, including apparent dependence on both force and muscle length. Also not included is extension (but not elastic energy storage) due to geometric factors [see Chapter 4 (Ettema and Huijing) for a quantification of these effects]. Of note is that if the curve shapes are not the same, the relative contribution between the subcomponents is a function of force (e.g., Stein and Gordon, 1986).

Isolated Tendon. Tendon properties are well documented, with the "toe" region (where the stiffness is increases approximately linearly with force, and thus is well represented by the classic exponential relation of *Eq. 5.3*) for about 3–4% extension, followed by a more linear region up to failure at about 7% (e.g. Butler et al., 1979). Although tendons possess viscoelastic properties, a high percentage (about 80%) of the stored elastic energy is recoverable for the typical physiological range of rates of loading (Alexander, 1988).

Tendon Extension with Muscle Contraction. Peak muscle-induced tendon extension is typically within 2–5% for most tendons [see Chapter 4 (Ettema and Huijing) and Chapter 36 (Alexander and Ker)]. The range of *in situ* applicability of the toe region, where the force-extension relation is nonlinear, is controversial. Based on assuming a factor of safety of at least 2 between the tendon failure load and the peak load generated by maximally contracting muscle (e.g., see Eliott, 1965), one would predict that typically a good portion of the tendon operating range during muscle contraction is within the "toe region" (see Figure 5.7). Indeed, some groups have found stiffness to increase (compliance to decrease) with increasing force for most of the range of loading [e.g., see Chapter 4 (Ettema and Huijing) for review of their work and that of Rack and Ross (1984)]. Winters and Stark (1985) assumed that peak extension was about 3-4%, and that for practical purposes this was within the toe region; thus they assumed an exponential relation. However, Morgan (1977) and Proske and Morgan (1987) suggest that tendon properties are linear above about 20% of

maximum isometric tension. Zajac's group (Zajac, 1989), emphasizing this data, utilize a linear relation from 20% force onward, and many groups assume a linear force-extension relation.

Simulation experience from thousands of runs utilizing various nonlinear and linearized models suggest that this assumption matters. Thus, further investigation is needed, primarily along the lines of Chapter 4. However, it appears that the findings presented in Chapter 36 (Alexander and Ker) may help resolve this issue. Here they divide musculotendinous systems into three categories: ***i)*** long muscle fibers with short tendons; ***ii)*** short muscle fibers with long, thin, extensible tendons (e.g. 4–5% extension with F_{max} applied); and ***iii)*** short muscle fibers with long tendons and larger cross sections than would appear necessary for a reasonable mechanical factor of safety (thus extending only about 2% with F_{max}). They postulate different uses for these tendons – in particular, ***ii)*** is best for elastic energy storage (e.g. many lower limb actuators) while ***iii)*** is better for control transmission and impedance modulation (upper limb). This helps explain some of my own concerns regarding predicted *SE* properties that I and my colleagues have estimated for about 80 muscles (e.g., Winters and Stark, 1988). For instance, assuming a similar peak tendon extension for all maximally contracting muscles (i.e. ratio of muscle to tendon cross-sectional area is uniform), we find that when converted to (more intuitive) joint units, the muscles surrounding the ankle joint in particular were quite stiff (e.g. soleus peak extension of only 19°) while those surrounding the wrist were quite compliant (e.g. half over 50° peak extension). This is due primarily to differences in moment arm. In retrospect, Chapter 36 and common sense suggests that the former, which are more involved in elastic energy storage and utilization, have relatively thinner tendons (see Chapters 33–37), while the latter, more involved in fine control and impedance modulation, likely have relatively thicker tendons (as suggested by the data of Rack et al., 1984).

Physical Sources Within Muscle. Jewell and Wilkie (1958) showed via direct observation that significant series extension existed within muscle tissue as well as within tendon. They also suggested that *SE*, and originally identified the Z-discs (and perhaps the actin filaments) as the most probable site. However, these are relatively short and would have to extend considerably for overall muscle extension to reach 4% (see form of *Eq. 5.7*). As suggested by Hanson and Huxley (1955) and Joyce and Rack (1969), it is now well accepted that part of the elasticity lies within the cross-bridge structure, likely including the *S1* bridge of myosin (e.g. Huxley and Simmons, 1971; Flitney and Hirst, 1978; Morgan, 1977). However, the range of strain proposed for the cross bridges [e.g. under 2% in Huxley and Simmons (1971) and up to 3% in Flitney and Hirst (1978), both relative to overall sarcomere length] seem small in comparison to data from whole muscle experiments (reviewed in Close, 1972). Evidence is also mounting that the myofilaments are also somewhat extensible [e.g., reviewed in Chapter 2 (Hatze); see also Chapter 4 (Ettema and Huijing); see Ford et al. (1977) for an alternate view]. Thus, ***all components of muscle appear to show some extension.*** In retrospect it would be surprising if such was not the case, especially since experimental investigations of whole muscle (often with little tendon included) have consistently found peak extensions of about 5% (reviewed in Close, 1972).

Relative Contribution of Each Component. What is the relative extension of the various contributions to series extension? Traditional input–output methods only measure a "lumped" value, but more recent techniques [see Chapter 4 (Ettema and Huijing)] allow more careful estimates. As reviewed in Chapter 4, for some muscles on the order of half of the *SE* extension is within muscle tissue (e.g. frog sartorius, cat soleus, human thumb). However, for many others, the majority of the *SE* extension of musculotendinous unit is due to the tendon. In a recent review article, Zajac (1989) suggested that, for most musculotendinous units, muscle series extension is virtually insignificant relative to tendon extension. When all put together, however, it seems evident that peak strains for both muscle and tendon are on the order of 3–5%, with only some of that within the muscle due to the cross-bridges.

Cross-Bridge Stiffness Vs. Passive SE. Based on intuition from molecular models (Section 5.3), the overall cross-bridge induced stiffness would be expected to increase as a function of the ***number of attached bonds.*** This is because cross-bridge stiffness can only be realized when the actomyosin complex is attached. This argument assumes an

idealized mechanical view of cross bridges in series and in parallel with each other, which is probably reasonable (Rack and Westbury, 1974). Each attached bond then contributes a "short-range" stiffness for about 2% of the sarcomere length (Huxley and Simmons, 1971, Rack and Westbury, 1974). Since the number of attached bonds is a function of calcium activation, the "short range stiffness" seen during ramp stretches differs from a passive series ***elastic*** element (Rack and Westbury, 1974). This is because a cross-bridge, after being broken, can ***reattach*** at a ***different*** (e.g. lengthened) actin site – it "forgot" that it was storing elastic energy relative to a certain rest length. This in turn also raise questions regarding the adequacy of the Hill-based model structure which will be addressed in Section 5.4.3.

Estimating SE/Stiffness in Humans. The classical "quick release" and "controlled release" approaches for isolated muscle are difficult to apply on intact human systems, due primarily to the confounding effects of large limb inertias (Goubel et al., 1971). Two very different approaches emerge:

1. Calculation Methods. This is based the isolated muscle data described above: peak muscle and tendon extensions are both about 3–6% strain, and a dimensionless "shape" parameter (Figure 5.7d) on the order of 3–5 provides a reasonable prediction of curve concavity. This ***material*** information, combined with estimated musculotendinous ***geometry*** [e.g., as cataloged in the Appendix (Yamaguchi et al.)], can be utilized to estimate ***structural*** values (e.g., Alexander, 1983; Winters and Stark, 1985).

2. Experimental Oscillation Methods. One set of approaches is based on applying small, fairly high-frequency oscillations about an otherwise steady isometric contraction against a bias torque. Either ***position oscillations*** [e.g., Joyce and Rack (1974); Zahalak and Heyman (1979), Ma and Zahalak (1987)] or ***force oscillations*** (e.g., Agarwal and Gottlieb, 1977) can be applied; the other of these becomes the measured output. The estimated stiffness, as defined by the peak-to-peak force change divided by the peak-to-peak position, changes as a function of the bias force in a way that appears to provide a stiffness measure that is essentially a good prediction of the *SE* over the entire *SE* range. Angular stiffness is almost linearly related to the bias torque, just as suggested previously for muscle and tendon over, at minimum, the lower force operating range.

Another class of approaches, which tend not to estimate the whole *SE* curve but rather a certain operating range, estimate stiffness from a measured ***resonance*** frequency; this may be determined from an "elastic bounce" record (e.g. Cavagna et al., 1971) or a "natural" voluntary rhythm (Greene and McMahon, 1979; Hof and Van den Berg, 1981, Bach et al., 1983).

It turns out that overall structural properties, as determined by these two methods, are in good agreement with each other for systems such as elbow flexion-extension, wrist flexion-extension, and ankle dorsi-plantar flexion (Alexander, 1983,1988; Winters and Stark, 1985,1988). Why do these methods tend to work? Because, as shown in Figure 5.8, for minor perturbations the *CE* works as a viscous, "soft" ground. Also, the changes in activation (as measured by the *EMG* fluctuations relative to the bias *EMG* level) are small and of sufficiently high frequency to be fairly filtered by muscle dynamic properties. Finally, activation and force are at about the same relative level, and thus if anything the curve concavity should be greater than that seen for quick release studies, as is seen.

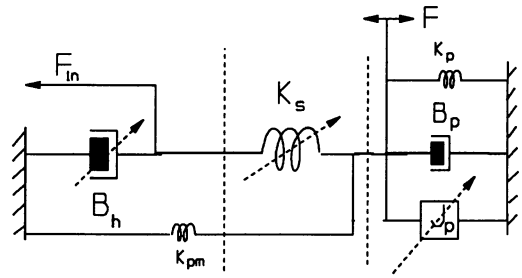

Figure 5.8: Muscle model isolating the series component but retaining gross properties to either side of the model. The lines through elements indicate sources of nonlinear influences.

Synthesis. The phenomena of variable series stiffness is admittedly a complex property that is not fully understood. In particular, the history dependence of series stiffness during dynamic movements, during which activation and force differ, requires further investigation, as do the effects of geometry. Nonetheless, there is a ***remarkable consistency*** between the information obtained by various methods, more so than generally recognized.

This important property is explicitly used in Chapters 1-6, 8-9, 17, 19-21, 30, 33-37, 41-43. These chapters, which span limb and torso sys-

tems, document a wide variety of consequences of series compliance, including: ***i)*** elastic energy storage; ***ii)*** modulation of operating ranges for the *CE*; ***iii)*** smoothing of movements; and ***iv)*** facilitation of dynamic stiffness/impedance modulation.

How should it be modeled? Possibilities include: ***i)*** a single linear spring element (used in many chapters); ***ii)*** a spring which an initial concavity followed over a large part of the operating range by a linear region (Zajac, 1989); ***iii)*** a traditional concave upward exponential curve, with a "shape" parameter of 3-5 (i.e., a linear relationship between stiffness and force); ***iv)*** a viscoelastic model including one of the aforementioned springs; ***v)*** a series connection of two (or more) nonlinear series springs (Stein and Gordon, 1986), perhaps with one spring modulated by force, the other via activation; and ***vi)*** a single stiffness value which is a weighted function of force and activation, with element extension determined via integration.

For those wanting a reasonable yet simple model, I suggest ***iii*** as opposed to ***i)*** or ***ii)***. In particular, linearization of this element, while often sufficient for studies of lower-limb elastic energy storage or unloaded upper-limb movements, should be avoided whenever one desires to use the model to gain insight into ***control*** aspects of tasks involving dynamic interaction with the environment. Recent (as yet unpublished) simulations by myself also suggest that adding a viscous component (model ***iv)***) has some interesting (yet subtle) consequences: ***a)*** a closer fit to quick-stretch and quick-release data (e.g. of Bagley, 1987); ***b)*** some capacity for showing history-dependent "force enhancement" tendencies (discussed later; see also Sprigings, 1986); and ***c)*** enhanced numerical stability of the muscle algorithm (which allows larger integration step sizes). The last reason alone is sufficient for employing a small damping element in optimization studies. Whether *SE* should be activation- and well as force-dependent requires further investigation by studies along the lines of Chapter 6 (Lehman).

5.3.3 The Contractile Element: Tension–Length and Force–Velocity

Two properties define this element: ***i)*** *CE* tension–length; and ***ii)*** *CE* force–velocity. After developing the basic relationships, we will look at how these relationships combine and how the *CE* element is influenced by activation. Special issues such as "yielding" are postponed until Section 5.4.1.

Active CE Length–Tension Relation

It has long been known that isometric muscle force development is a function of length (e.g. discussed in Gasser and Hill (1924); Ramsey and Street (1940), Ralston et al. (1949)), with the muscle force maximum at an intermediary ("optimum") length (about 1.05 times the "rest" length) and lower for shorter or longer lengths, finally reaching near zero at about 0.4 and 1.5 times the resting length, respectively (e.g., Figure 5.9). Thus the slope, a measure of static stiffness, includes both positive and negative (potentially unstable) ranges. The lack of an abrupt end of force near zero force locations is likely due to cross-bridge non-uniformity [see also Chapter 3 (Morgan)].

Since the 1950s, isolated muscle *CE* tension–length and human joint moment–angle curves have been available within the literature for the special case of maximal activation and maximal effort, respectively [e.g. review by Kulig et al. (1985)]. Using techniques that allowed measurement at the microscopic level, Gordon et al. (1966) showed conclusively that this fundamental property was due to the amount of overlap between thick and thin filaments, as predicted by the sliding filament theory [Chapter 1 (Zahalak)]. A wide variety of empirical fits have been utilized to characterize the basic behavior.

The physiological operating range is always much less than the full range; that shown in Figure 5.9, with a positive slope over most of the *in situ* muscle range, is typical. However, there are notable exceptions (e.g. knee and elbow extensors).

Of note is that the curve shape for the *CE* is ***not*** the same as that for the whole muscle (e.g., see Figure 12 in Zajac, 1989 and Figure 5.10). This is because the extension of *SE* is a function of force, and the force is not constant . For this and perhaps other reasons (see Hatze, 1981), the musculotendinous "tension–length" curves for isometric twitches (about 15–30% of tetanic force) and those for isometric tetanus should also not be expected to be simple multiplicative scales of each other.

Two important practical questions remain:

1. Determination of in situ rest length. This is hard to estimate because most joints are crossed by multiple muscles. Figure 5.9 provides an example of simulation predictions of how *CE* tension–length and subsequently joint torque–angle relations change as the assumption of rest length changes. By making such

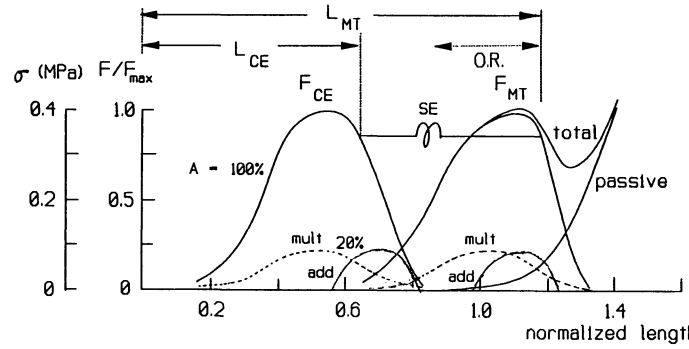

Figure 5.9: Idealized tension–length for tetanic (maximal) contraction (solid lines), as seen across the *CE* element (to left) and whole musculotendon unit (to right). This difference between the two is the extension of the *SE*. Family of tension–length curves with submaximal activation (here 20%) may assume multiplicative scaling (dashed lines) or additive scaling (solid lines). Also shown are stress units, with the maximal stress about 0.3–0.4 MPa, and to a first approximation is independent of fiber composition.

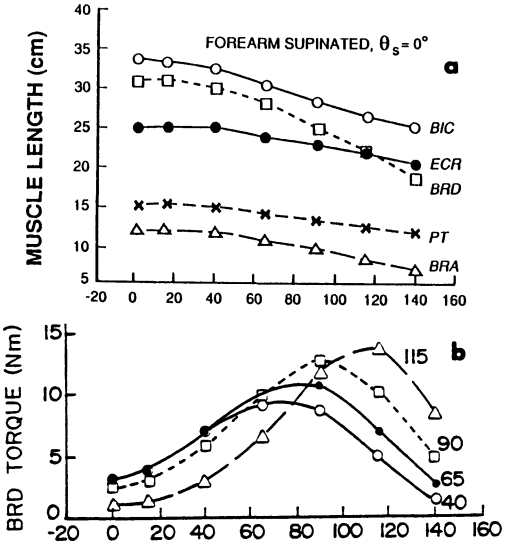

Figure 5.10: *a)* Sensitivity of muscle length to joint angles, here for elbow flexors as a function of elbow flexion angle. *b)* Changes in the simulated maximal isometric torque-angle relation as a function of the assumed muscle rest length, shown here for the brachioradialis (*BRA*). For the extended positions a curved (spherical arc) approximation was employed [method reviewed in Section 8.2.4 of Chapter 8 (Zajac and Winters)]. (Adapted from thesis by Kleweno, 1987).

predictions for all muscles and comparing to experimental data, rest lengths can be estimated (Kleweno and Winters, 1988).

2. CE tension-length curve for submaximal activation. This is less well documented and more controversial. Based on purely mechanical considerations, since *SE* extension increases with force and thus (usually) activation, the curve peak for whole muscle might be expected to shift toward longer lengths as the steady activation level increases. Modeling assumptions may assume that the *CE* (or whole muscle) curve scales downwardly as a multiplicative factor, essentially modulating stiffness (e.g. Winters and Stark, 1985; dashed line in Figure 5.8) or that it shifts downward and to the right or left (dotted line in Figure 5.8). Notice that for lower activation levels the passive (parallel elastic) component has a relatively larger influence. These poorly understood subtle differences are especially important in relation to the theories of motor control discussed in Chapters 11–17.

CE Force–Velocity Relation.

Four classical methods have been utilized to experimentally estimate this behavior: ***i)*** Isometric-to-isotonic contraction (afterloaded); ***ii)*** isometric-to-isotonic contraction (not afterloaded); ***iii)*** isometric contraction dynamics (requires knowledge of *SE*); and ***iv)*** isokinetic contraction.

Since first used by Fenn and Marsh (1935), isotonic methods (fortunately) dominated the early work. Ideally, measurement should be made at a specified position while the muscle force and velocity are ***constant***, i.e. their derivatives (slopes) are zero. The classic isotonic studies of the human flexors by Dern et al. (1947) and Wilkie (1950) provided strong evidence in support of the basic Hill model structure, and further documented shapes of the force-velocity relation that were consistent with the Hill relation, especially once an estimate of the effects of forearm inertia is subtracted out.

Although related to muscle energetics by Hill, the *CE* force-velocity is essentially just a fit to experimental data. This relationship has been estimated by many groups, with the vast majority finding data compatible to the Hill hyperbola.

Other proposed force–velocity relations include:

$$F_{ce} = F_{max}\, e^{-a v_m} - b\, v_{ce} \qquad (5.8)$$

[Fenn and Marsh (1935)]

$$F_{ce} = F_{max}\, e^{-(F_{ce}\, v_{ce} / b F_{in})} - V\, a/b \qquad (5.9)$$

[Abbott and Wilkie (1953)]

$$F_{ce} = F_{max}\, e^{-a v_m} - b\, l_{ce} \qquad (5.10)$$

[Aubert (1956)]

where a and b are different constants in each case and F_{max} is the peak isometric force; all have three describing parameters.

Hatze (1981) has proposed an additional relationship in which the concavity of the curve changes for small shortening velocities (which is not true for the Hill hyperbola); it is too complex to present here. His rationale was the data of Edman et al. (1976), which suggested that a concavity occurred around 80% of the isometric force; Cecchi et al. (1984) presents similar results. Furthermore, a number of similar shapes have been obtained for human systems, primarily for knee rotation experiments utilizing isokinetic machines (e.g. Perrine and Edgerton (1978)) and wrist rotation (Baildon and Chapman, 1983). Reasons for these differences are unknown; however, many curve shapes can be estimated from the same human testing data set, especially for "isokinetic" testing (Yates and Kamon, 1983; Winters and Bagley, 1987). In fact, I have found that students presented with isokinetic "dynanometer" input–output data from a ***model*** which ***includes*** a Hill-based *CE* will produce a variety of curve estimates! Also, Zahalak et al. (1976) have shown that *EMG* activity tends to grow for slow shortening velocities; this may also help explain part of the human data. The fundamental problem is that *CE* tension–length, *SE*, *PE*, system inertia and activation all represent confounding influences. Results not following a Hill-like shape must be contrasted with the dozens of results, ranging from isolated fibers through whole muscle to muscle joint systems, where the Hill hyperbola has been a good fit for shortening muscle. Lengthening *CE* force–velocity behavior will be addressed further in Section 5.4.1-2.

The Hill hyperbolic relation has remained the standard not just because it adequately approximates a wealth of experimental data but also because the ***describing parameters are intuitive.*** The dimensionless parameter a_f defines the hyperbolic shape and the parameter CE_{vmax}, the maximum unloaded *CE* velocity, defines velocity intercept (see also Figure 5.2). The last parameter, which describes the force intercept, is the hypothetical isometric force, which we will see comes from the *CE* tension-length relation. This relation can be rewritten into many forms, including (Wilkie, 1956):

$$\left(a_f + \frac{F_{ce}}{F_{max}}\right)\left(a_f + \frac{v_{ce}}{v_{max}}\right) = a_f + 1 \qquad (5.11)$$

One could also divide by a_f. Other normalized forms are (e.g., Fung, 1981; note symmetry):

$$\frac{v_{ce}}{v_{max}} = \frac{1 - (F_{ce}/F_{max})}{1 + (F_{ce}/(F_{max} a_f))} \qquad (5.12)$$

$$\frac{F_{ce}}{F_{max}} = \frac{1 - (v_{ce}/v_{max})}{1 + (v_{ce}/(v_{max} a_f))} \qquad (5.13)$$

To show explicitly that this equation describes the behavior of a force generator in parallel with a dashpot, as in Figure 5.11, the following form can be utilized [e.g. Cook and Stark (1968)]:

$$F_{ce} = F_{in} - B_h\, v_{ce} = F_{in} - \frac{F_{in}(1+a_f)}{a_f\, v_{max} + v_c}\, v_{ce} \qquad (5.14)$$

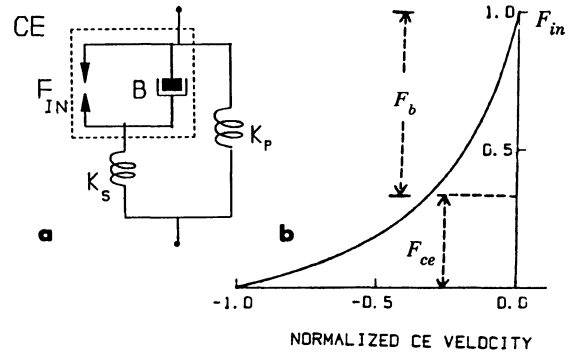

Figure 5.11: ***a)*** Hill model structure showing *CE* divided in a parallel dashpot representing force "lost" via the force–velocity relationship and a *CE* "sculpturing" product relationship for the *CE* tension–length relation. ***b)*** Explicit view of the force "lost" and the force "passed".

It is worthwhile to provide ***material*** property estimates for the two intercept parameters. In this way one can easily extend the results to ***structural*** properties by combining the materials properties with certain geometric features such as physiological cross-sectional area, pennation angle, and

length (Winters and Stark, 1985; Zajac, 1989). The experimentally verified range for a_f is approximately 0.1 to 1.0, with slow muscle fibers between 0.1 and 0.25 and fast fibers greater than 0.25 (e.g., reviews by Close, 1972; Winters and Stark, 1985). CE_{Vmax} ranges from about 2 L_o/sec (muscle fiber lengths per second) for slow fibers to about 8 L_o/sec for fast. The composition of most muscles is mixed, and thus most muscles are between these extremes, and can be estimated by a linear functions of muscle fiber composition (Winters and Stark, 1985). Thus, using the Hill approach, the only new parameter needed to adequately describe muscle ***material*** properties is ***muscle fiber composition***. Structural properties for a given musculotendinous unit of course scale with muscle geometry.

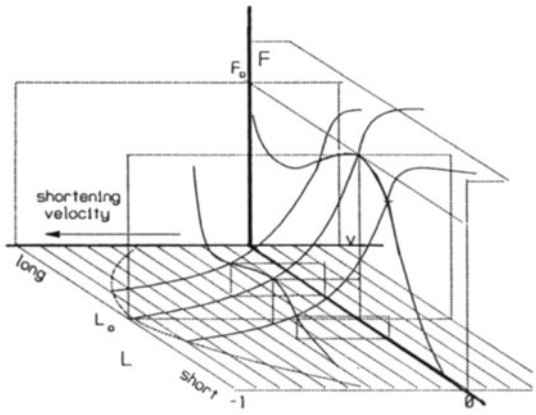

Figure 5.12: Three-dimensional view of the *CE* behavior for a certain activation level, showing a few cases for different lengths and velocities.

Interaction Between CE Tension–Length and CE Force–Velocity. The studies of Abbott and Wilkie (1953) for isolated frog muscle provided the conceptual foundation for allowing $F_{fv\text{-}in} = F_{tl\text{-}out}$, i.e. the *CE* force–velocity input force (*y*–intercept) equals the *CE* tension-length output (see also Figure 5.12). They also suggested that the parameters a_f and b (and thus v_{max} in Hill's equation) remained constant. These observations were supported by Bahler (1968) and are now a standard assumption. A three-dimensional force-velocity-length curve can be utilized to describe this relationship [Bahler et al. (1967), Partridge (1979), Figure 5.12]. Mathematically, this takes the form (e.g., from *Eq. 5.11* and *Eq. 5.14*, respectively):

$$F_{ce} = \frac{a_f\ (1 - (v_{ce}/v_{max}))}{a_f + (v_{ce}/v_{max}))}\ F_{fvin} = \left[1 - \frac{1 + a_f}{a_f v_{max} + v_h}\right] F_{fvin} \tag{5.15}$$

Notice that these forms display a ***product*** relationship between the two phenomena (assuming maximal activation for present):

$$F_{ce} = F_{fv}(v_{ce}, F_{fvin}) = F_{fv_1}(v_{ce}) * F_{tl_1}(L_{ce}) = F_{fv}(v_{ce}) * F_{tl}(L_{ce}) * F_{max} \tag{5.16}$$

where $F_{fv}(v_{ce})$ and $F_{tl}(L_{ce})$ are dimensionless functions, each defined by two parameters. This shows that *CE* properties are best ***not*** represented by a parallel arrangement of a spring and dashpot – in such a case the relation would be additive [see also Figure 21.5 in Chapter 21 (Crago et al.)].

Scaling of Force-Velocity Parameters with Length. A_f is traditionally considered to be independent of length. Bahler et al. (1967) found that with maximal activation CE_{Vmax} peaks within the mid-operating range and drops off a shorter lengths where cross-bridge overlap is less. Data by Edman et al. (1968) on frog muscle fibers suggests relatively constant value over a medium range of lengths, a low value at small lengths, and a higher value at long lengths. However, over the typical physiological range of length changes (e.g., sarcomere lengths of about 5.8 to 2.8 μm), the value is relatively constant and probably consistent with the results of Bahler et al. Thus, variation with length over the physiological range appears marginal.

Scaling of the CE Force–Velocity–Length Relation with Activation. A question that the early pioneers had to address was how to modify *CE* force–velocity behavior at sub-maximal activation and muscle length. Wilkie (1956), summarizing frog data, and Bigland and Lippold (1954), using human calf muscle *EMG* measurement as an estimation of activation, suggested that the F_{fvin} parameter in the Hill equation could be scaled with activation, with the curve shape parameter (a_f) and the maximum velocity

parameter (CE_{vmax}) remaining about the same. (However, the data of Bigland and Lippold (1954) for human calf muscles lacked data above about 40% of CE_{vmax}). The data of Bahler et al. (1967) further refined these concepts, which can be viewed as follows:

$$\frac{F_{ce}}{F_{max}} = F(A, l_{ce}, v_{ce}) = A * F_{max} * F_{tl}(l_{ce}) * F_{ce}(v_{ce})$$

where A is the normalized activation. Notice that the normalized CE length–tension and CE force–velocity effects are effectively decoupled (shown orthogonal in Figure 5.12), and that for a given activation, the relation is assumed ***instantaneous***, i.e. statically satisfied. Furthermore it is still a ***product*** relationship. Notice that there are four interrelated variables: activation A, CE length L_{ce}, CE velocity v_{ce}, and muscle force F_m. If ***any three*** of these variables are known, the other can be determined. For example, if muscle force is unknown: ***i)*** A "sets" the CE tension–length relation, ***ii)*** given this relation, the "hypothetical isometric force" (F_{tlout}, which equals F_{fvin}) is read off from the appropriate length; ***iii)*** F_{fvin} the CE force-velocity curve; and ***iv)*** finding the appropriate CE velocity, the muscle force is read off. If activation is unknown: ***i)*** given F_m and v_{ce}, F_{fvin} is determined; ***ii)*** given an estimate of l_{ce} and F_{tlout} ($= F_{fvin}$), A is estimated.

Of note is that care must be taken if one chooses instead to represent the CE tension–length property by a spring in parallel with the force–velocity dashpot: the resulting CE then has dynamics, and thus the CE force–velocity–length relation is no longer instantaneous. Additionally, because the dashpot is traditionally assumed to be a function of F_{fvin}, force–velocity determination becomes awkward.

Is the parameter CE_{vmax} constant with activation? Some groups (e.g. Hatze, 1981; Audu and Davy, 1985) have followed the traditional line that says that it doesn't change with activation. However, Julian (1971) shows that this parameter is a function of the calcium concentration. On theoretical grounds, Julian and Sollins (1973) suggest that the level of activation affects the Huxley rate constant for breaking bonds which are opposed to shortening; this, in turn, affects CE_{vmax}. Both Zahalak et al. (1976, human elbow flexion) and Petrofsky and Phillips (1981; cat medial gastrocnemius) found that this parameter does scale significantly with activation. Of note is that some scaling would be expected for a muscle with mixed fiber composition due to the assumption of an orderly recruitment of motor units (Henneman, 1965): ***slower*** muscle fibers are more likely to be active during ***low*** activation, with faster fibers ***recruited*** as activation increases (Winters and Stark, 1985). This suggests that for mixed-composition muscle (the majority) this parameter ***should vary***, but perhaps not as significantly as F_{fvin} (e.g. as in Figure 5.13c). For instance, Winters and Stark (1985) assume as a default that CE_{vmax} drops at half the rate of F_{fvin}. Notice that if CE_{vmax} varies linearly with F_{fvin}, the relative shape of the force–velocity relation is independent of activation.

Zajac (1989) suggested that since the high-velocity region is of little practical importance for *in situ* functioning systems, the assumption for CE_{vmax} may not be of practical importance. Consider, however, the vertical lines in Figure 5.13, where for a given CE velocity (representing the low-velocity range of great practical importance), the assumption for CE_{vmax} affects not only the absolute force, but also the slope (and thus the instantaneous dashpot value). Also drawn in are the slopes connecting the intercepts, which have been utilized often as a mode of linearization (e.g. Baildon and Chapman, 1983; Zajac, 1989). Note that the intercept slopes and the curves slopes are ***not*** one-to-one, even though the same dimensionless shape parameter is assumed. This shows how difficult (and dangerous!) linearization of the force–velocity relation can be; if truly necessary, it is best accomplished uniquely for ***each task*** of interest [Seif-Naraghi and Winters, 1989)].

Is the Force–Velocity–Activation Relation "Instantaneous"? This question considers whether or not the force–velocity relation is satisfied at every instant, given an appropriate activation input. If so, the relation is static, and thus not history-dependent. (Of course, the overall model still produces history-dependent behavior due to the interaction between elements.) Jewell and Wilkie (1958) concluded that in frog sartorii a change in velocity follows a change in force very quickly ("probably in less than 1 msec, certainly in less than 6 msec"). Hill investigated this in more detail using various strategies, including both isotonic and isokinetic, and came to the conclusion that, for all practical purposes, the relation is uniquely satisfied for shortening muscle at each instant. The human elbow flexion data of Pertuzon and Bouisset (1973) provide further support for

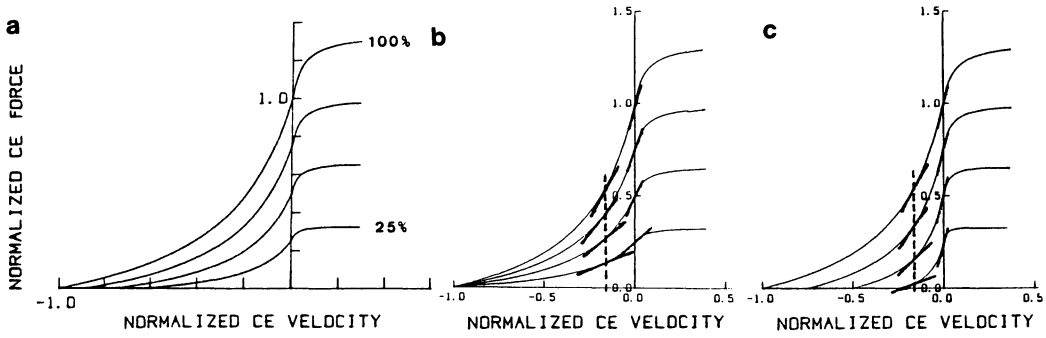

Figure 5.13: Maximal and submaximal *CE* force–velocity curves for assumptions of a variable versus an activation-independent $CE_{v_{max}}$ parameter. *a)* Default approach used by the author. *b)* and *c)* Two extreme approaches used in the literature. Notice that this assumption does make a difference, both for moderate velocities (mostly magnitude effect) and near zero velocity (mostly slope effect).

this assumption. It clearly is not satisfied for lengthening muscle (e.g. Joyce and Rack, 1969). (However, if "attachment" replaces "activation" as the input to the *CE*, as recommended in Section 5.3.1, then perhaps it might still be satisfied [Winters (1989)].

5.3.4 Excitation–Activation Dynamics from the Hill Model Perspective

In this section we cover material also presented in Chapter 1 (Zahalak), only from the "input–output" systems perspective characteristic of the Hill model approach. Activation dynamics is first covered; this is followed by the treatment of how *CE* is usually scaled by activation.

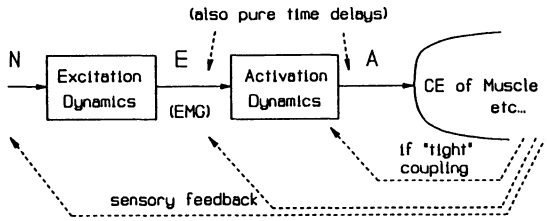

Figure 5.14: Block diagram of relationship between excitation, activation and muscle mechanics.

"Active State" and "Calcium Activation"

Hill (1949) defined the "active state" as the tension that the *CE* would generate, without lengthening or shortening, after the beginning of excitation. He considered activation to be virtually instantaneous, with deactivation a much slower process. An activation "plateau" was often seen. The time course of the falling phase of the "active state" could be estimated experimentally [see Close (1972) for review]. As seen in Figure 5.14, activation is thus considered as the ***output*** of the excitation–contraction coupling dynamics and the input to *CE*. In 1960 Jewell and Wilkie questioned the concept of the active state, in particular as related to its assumed length-independence. Others, such as McCrorey et al. (1966), wondered whether some of the differences between series elastic and force–velocity relation obtained by isotonic versus isometric methods might not be due to active state assumptions.

In 1968, based on studies of the rate-limiting role of calcium in the muscle activation process, Ebashi and Endo defined the active state as the ***relative amount of calcium bound to troponin.*** This concept, since modified to represent evolving information on bonding site physiology [see Chapter 1 (Zahalak)], found immediate acceptance [e.g., Julian and Sollins (1972), Hatze (1974)], and is now a common conceptual (though immeasurable) assumption for Hill-based models.

For physiological temperatures, the data of Bahler et al. (1967) suggested an activation time on the order of 10 msec and deactivation on the order of 50 msec, and that active state dynamics could be adequately represented by a first-order system. Thus the simplest approach for modeling this dynamic process has been to assume unidirectional flow and first-order dynamics in which either the activation time constant is constant

(linear model) or there are two time constant values, one for lengthening and one for shortening [e.g., Cook and Stark, 1958; Lehman and Stark, 1979; Hof and Van den Berg, 1981; Winters and Stark, 1985; Zajac, 1989]. Winters and Stark (1985) suggest that these time constants are a function of the muscle fiber composition (higher time constants with slower muscle fibers) and muscle size (higher time constants in larger muscle volumes). Ma and Zahalak (1987) and Zajac (1989) have suggested first-order nonlinear dynamics in which the time constant is variable (Section 5.7). Hatze (1981) assumes second-order dynamics for this excitation–activation relation.

Is muscle activation truly uni-directional, independent of muscle dynamics? Indirect evidence from experiments in muscle mechanics (e.g., Bahler et al., 1967; Rack and Westbury, 1969) suggests that it may be a function of length. Experiments by Fuchs (1977) suggested that calcium–troponin interactions may be coupled with actin–myosin interactions. Such observations prompted Ma and Zahalak (1987) to formally distinguish between the two possibilities by referring uni-directional coupling as ***"loose" coupling*** and bi-directional coupling as ***"tight" coupling*** [Chapter 1 (Zahalak)].

Of note is that the "loose" coupling assumption is compatible with ***any*** muscle model, and thus when employing this assumption ***one can "mix and mesh" models of activation with models of muscle mechanics***. An example in the *PEXA* model of Hannaford that is described in Chapter 7 (Hannaford and Winters). However, combining an activation model with Hill-based models is not as theoretically elegant as it is when using the molecular models.

Excitation, Effort, and Neural Dynamics

As seen in Figure 5.14, excitation is defined here as the input to activation dynamics. Conceptually, the output of excitation dynamics can be thought of as similar to a lightly filtered, rectified *EMG* (Winters and Stark, 1985; Gottlieb et al., 1989; Chapters 14-15, 19). If muscle is electrically stimulated or the model input is an *EMG*, excitation dynamics are of no interest. However, in most simulation studies an idealized input representing the *CNS* output, such as a pulse, is assumed that differs in shape from an *EMG*. Excitation dynamics heuristically represents the very real fact that neural dynamics may be part of the rate-limiting process. Such dynamic effects may include recruitment, the finite time nature of firing rate, any "smoothing" effects in the lower circuitry, and the simple fact that higher brain signals are not idealized. It may be modeled as a first-order filter (Hatze, 1981; Winters and Stark, 1985). Often excitation has been assumed to be negligible, especially when considering eye movements (e.g. Cook and Stark, 1968; Lehman and Stark, 1979).

Chapman and Calvert (1979) have suggested that perceived "***effort***," similar in concept to the "excitation" input, is fairly consistent between subjects. Our data with submaximal exercise (Silver-Thorn and Winters, 1988) suggests that subjects correlate perceived effort with force rather than *EMG*. This interesting concept needs to be further explored.

Hatze (1977, 1981) has separated out "recruitment" and "firing rate" effects. Although theoretically elegant, the latter approach is practically difficult since there are now two inputs per muscle, and it is difficult to separate out the two effects when using surface *EMG* electrodes. Nonetheless, his approach deserves further study, both for theoretical investigations and for studies related to muscle fatigue (e.g., due to muscle stimulation).

5.4 Challenges for Hill-Based Models (and Suggested Strategies)

In this section we deal with three classes of experimentally measured history-dependent phenomena that are difficult to describe within the context of the traditional Hill-based model structure: ***i)*** "yielding" during lengthening; ***ii)*** "force enhancement" after stretch; ***iii)*** subtle stiffness effects.

The concept of "***attachment***" (rather than "activation") as an input to the Hill-based contractile machinery is introduced as an approach for partially dealing with such phenomena. Additionally, it is suggested that passive mechanical sources for certain phenomena have not always been adequately addressed. Finally, it is shown that some of these phenomena are seen only in experiments of little relevance during normal human movement tasks.

5.4.1 Lengthening Muscle

It is well documented, at least for ramp stretches within certain muscles (e.g. cat soleus), that lengthening muscle exhibits history-

dependent behavior that is incompatible with the classical *CE* activation–force–velocity–length approach of Figure 5.12 (Joyce et al., 1969; reviewed in Chapters 1–3). However, other muscles display a force saturation with little yielding (e.g. cat medical gastrocnemius); these muscles can be adequately approximated by a lengthening *CE* force-velocity fit.

The fact that the *CE* element in Hill-based muscle models is assumed to be instantaneous and single valued is one of the primary criticisms of such models (e.g., Zahalak, 1981 and Chapter 1). This is indeed a weakness. Most current *CE* force–velocity relations assume a saturation with progressively lengthening velocities at about 1.3 F_{max} (e.g., Hatze, 1981; Winters and Stark, 1985; see also Figures 5.2 and 5.12); however, values as low as 1.1 F_{max} [Chapter 36 (Hof and Van den Berg), experimentally estimated for ankle muscles] and as high as 1.8 F_{max} [Chapter 6 (Lehman)] have been used. Additionally, most models assume that the slope at low lengthening velocities is higher than that are low shortening velocities.

Of note is that most of the evidence for yielding unfortunately comes from experiments where the muscle is originally under ***steady*** activation for a significant period of time. The data of Cordo and Rymer (1982) indicate that yielding does not occur in ***newly recruited*** muscle fibers. This is of great importance since it suggests that the muscles causing changes in movement direction (involved in a "stretch-shortening cycle") are likely not to yield. On teleologic grounds alone this might be expected (Winters and Stark, 1987), especially given the proficiency of tasks in life (e.g. walking, running, kicking) which involve stretch-shortening muscle behavior.

Yielding is also is a function of ***how*** the muscle is transiently lengthened. For example, yielding is not seen below a certain velocity threshold, and furthermore sudden isovelocity ramps appear to cause more yielding than isotonic loads which induce lengthening [compare Joyce et al. (1969) to Joyce and Rack (1969)]. Of note is that because of the inherent inertia of musculoskeletal systems, the idealized isokinetic "hold-to-ramp" transition that induces yielding is not a good approximation of *in situ* human movements, except for tasks involving unexpected "impacts". Here is where yielding might be most expected. Anticipated impacts may also show yielding (e.g. striking a ball with a bat; kicking or hitting an object; being struck by an object).

A number of modeling approaches have been used to simulate yielding which take advantage of insights from Huxley-based molecular models, but without their complexity. Van Dijk (1978), representing the Huxley model by 3 differential equations, used a "compromise" lengthening force–velocity curve that had a high force-velocity slope for velocities under about 0.2 times V_{max}, then yielded dramatically. Crowe et al. (1980) provided a length-dependent feature by dividing attachment locations into 4 length "bins". They found reasonably good correlation to their experimental data. The most theoeretically elegant approach, the Distribution Moment (*DM*) model of Zahalak (1981), is covered in Chapter 1. Here we consider a conceptually different approach that allows the Hill model to remain intact.

"Attachment" as the Input to the CE

Based initially on a "challenge" from George Zahalak, I recently developed a class of approaches for approximating "yielding" behavior from within the confines of Hill-based models (1988, 1989). Central to the conceptual foundation is a ***distinction between "activation" and "attachment."*** It is assumed that the "problem" with simulating yielding is not an inadequate *CE* model but rather an inadequate estimation of attached bonds; the instantaneous, single-valued *CE* relation is assumed to still hold for ***those bonds that remain attached.*** Attachment, the input to the *CE* element, is thus a function not only of the ongoing activation, but also the rate-of-change of activation and *CE* dynamics. Somewhat surprisingly, a number of heuristic relations were formulated that provide reasonably good simulations of this behavior. All involve increasing the order of the model by one due to the addition of a nonlinear first-order process relating attachment to activation. All start by assuming that at each instant the "attachment" (A_{att}) differs from the "activation" (A_{act}) by a history-dependent yielding function (F_y):

$$F_{att}(A,v_{ce}) = F_{act}(A) - F_y(A,v_{ce}) \tag{5.18}$$

The form of F_y used in Winters (1989) is:

$$\tau \dot{F}_y + F_y = \begin{cases} \left[\frac{v_{ce}}{v_{max}}\right]^{0.5} \left[\frac{kF_a + F_{max}}{k+1}\right] \{1-(\dot{A}/\dot{A}_{max}\} & v_e > v_{cr} \\ 0 & v_e \le v_{cr} \end{cases} \tag{5.19}$$

where:

$$\tau_y(A,v_{ce}) = \frac{\tau_{yo}}{1 + (v_{ce}/v_{max})} \qquad (5.20)$$

Eq. 5.19 ***empirically*** combines into a product relationship three experimental observations (from left to right in *Eq. 5.29*): ***i)*** yielding increases as lengthening increases, with there being a "threshold" below which yielding does not occur (Joyce et al, 1969)); ***ii)*** the amount of yielding is inversely proportional to the current activation level; and ***iii)*** the amount of yielding is greatest with steady or decreasing activation and is nearly non-existent when muscle is increasing in activation (Cordo and Rymer, 1982).

Although the *CE* relation is ***remains instantaneous*** and single valued, a schematic of what the history-dependent range would have been if the $F_{fv_{in}}$ due to attachment was replaced by that which would have occurred due to activation is illuminating. Such a plot is shown in Figure 5.15.

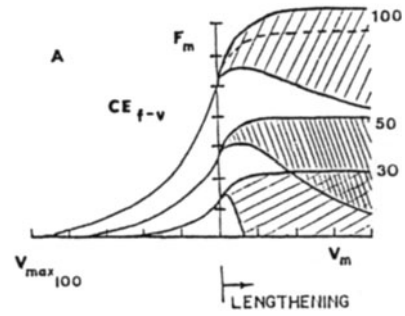

Figure 5.15: Schematic identifying of range of possible lengthening behavior *if* the *y*-intercept $F_{fv_{in}}$ due to activation were to replace that due to attachment (which is actually used). Three hypothetical activation levels are shown. The location within these ranges at a given time is history-dependent.

This distinction allows classic nonlinear "yielding" phenomena, as described by Joyce et al. (1969), to be closely simulated within the context of a Hill-based model structure that retains the instantaneous *CE* force–velocity–length element (Winters, 1989) and the *CE–SE* model structure. Figure 5.16a provides a dynamic example of how attachment differs from activation and consequently affects model performance; Figure 5.16b provides a summary of the observed model "ramp-and-hold" behavior, while Figure 5.16c shows that appropriate simulation of the sinusoidal oscillation data of Joyce et al. (1969). The latter case addresses another criticism of Hill-based models, showing that, with our "attachment" approach, the average force (and for low activation even the peak force) can in fact fall below the isometric force (Figure 5.16b).

Our own investigations of lengthening muscle behavior in humans, concentrating on the "strategic" low-to-moderate velocity range, have produced mixed results. In a very careful study of alternate isokinetic-isometric (repetitive ramp-hold-ramp) sequences during "steady maximal" (perhaps 90% effort) elbow flexion, in which the effects of *CE* tension–length-related "drifts" were carefully isolated out, Bagley (1987) saw little yielding in most subjects but a definite indication of a change in *CE* force-velocity slope with increasing velocity (Figure 5.17a). Yet Silver-Thorn (1987), employing ***submaximal*** effort levels

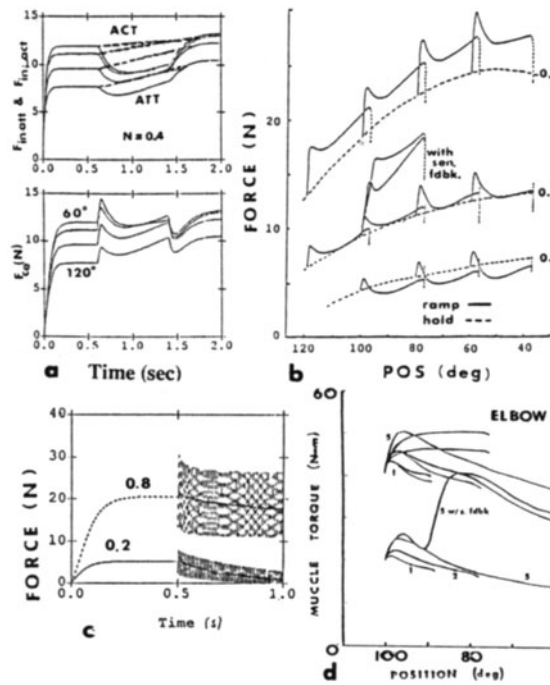

Figure 5.16: Summary of simulation results of classical cat soleus data displaying "yielding" and for elbow flexion. ***a)*** Muscle activation (dashed), attachment (solid) and force trajectories during a typical ramp-and-hold simulation. ***b)*** Summary of cat soleus force-position data for an assortment of "ramp-and-hold" experiments (compare to Figure 3 of Joyce et al., 1969). ***c)*** Cat soleus model response to 100 Hz vibration for two different initial activation levels. ***d)*** Elbow flexion ramp-and-hold simulations for two initial bias torques and in each case for speeds between 1 and 5 rad/sec. Top traces includes two parameter sets, one causing yielding and one not. Notice for both ***b)*** and ***d)*** that activation increases due to sensory feedback eliminated most of the yielding effect.

during cyclic isokinetic exercises of knee musculature, saw consistent, repetitive indications of yielding in ***some*** subjects (Figure 5.17b) that were clearly not due to changes in effort levels or reflex activity (as seen via *EMG*s). Others showed no such signs whatsoever. These preliminary observations suggest that there is ***variability*** in the amount of yielding seen in different subjects performing the same tasks. This makes modeling more difficult. It also suggests to me that one of the primary differences between "great" athletes and the rest of us may be related to the capacity to control yielding: yielding is undesirable during activation of a lengthening agonist undergoing "stretch-shortening", yet it is desirable to have quick yielding in an antagonist undergoing deactivation (e.g., see Figure 5.18).

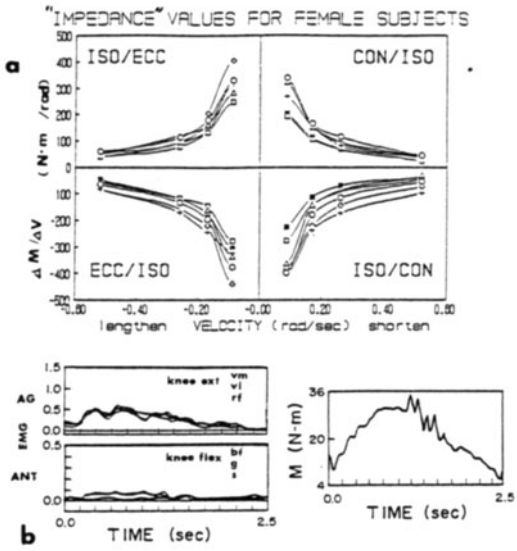

Figure 5.17: Sample results from experiments searching for yielding in humans. ***a)*** Summary of change in torque versus change in velocity (impedance units but not a true measure of impedance) versus Kincom (Chattecx) isokinetic velocity setting during the initial 80 ms intervals for eccentric⟷isometric and concentric⟷isometric transitions. Results for female subjects and for the "female" muscle-joint model (**a**) are shown here; results for males were very similar, only with "impedance" values nearly twice as high for all velocities. Adapted from Bagley (1987). ***b)*** Typical low-velocity experimental data which showed "yielding" during isokinetic knee extension movements (adapted from Silver-Thorn, 1987). The bell-shaped base in the torque curve is an artifact of start-up effects and the *CE* torque-angle property. Notice also the damped torque oscillation; this was typical.

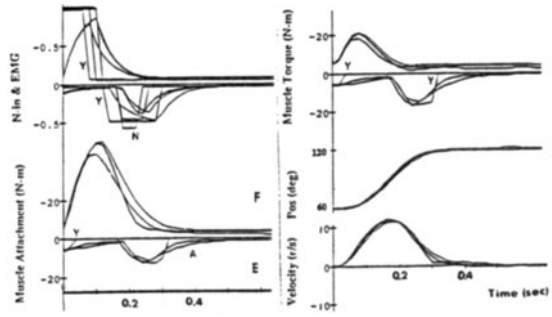

Figure 5.18: Model results for tasks with similar position trajectories but with and without the "attachment-yielding" addition to the model. With this addition, the antagonist "turns off" more quickly than with the default model, and consequently the agonist pulse width can be less. However, a larger antagonist "clamping" pulse was required for the yielding case.

Does this new approach "solve" the problem of simulating muscle yielding within the context of the Hill-based model? Yes and no. On the positive side, it provides a conceptual foundation for simulating yielding phenomena while retaining the Hill-based model structure and properties; "attachment" simply becomes the input to *CE*. On the negative side, it is a totally heuristic approach. Additionally, unlike parameters for shortening muscle or the other relations that have been discussed, we have not uncovered a systematic, rational basis for determination of task-independent parameter values for a range of muscles. Of course, our experimental data suggests due to muscle yielding variability this might be futile anyway.

5.3.2 "Force Enhancement"

Another phenomenon of muscle that has traditionally been difficult to model via Hill-based (and Huxley-based) models is force enhancement (Abbott and Aubert, 1951; Sugi, 1979; Edman et al., 1978; Julian and Morgan, 1979). When isometric conditions are reestablished after stretching a muscle (the "ramp-and-hold" protocol), the isometric force generated tends to be higher than that which would be seen for a normal isometric contraction under the same activation level and initial length. This phenomena is most likely when the muscle is at a length longer than the optimum length [Edman et al., 1978; see also Chapter 3 (Morgan)]. It is an open (and controversial) question regarding how "permanent" this "extra" force is, with some groups claiming that it is (Hill, 1977), while others suggest that it continues to decay for at least 1.5 seconds and eventually disappears (Van Atteveldt and Crowe, 1980). Although Sugi (1979) at-

tributes this excess tension to forces exerted by cross-links that are "locked out" at small displacements, this phenomenon is difficult explain via traditional cross-bridge models (Edman et al., 1978; Atteveldt and Crowe, 1980).

Can this phenomenon be seen in human data? The data of Gielen and Houk (1987; wrist movements) show that it exists for at least a few seconds. In our investigations of maximal isometric force levels following slow lengthening of maximally contracting elbow flexors, we have seen clear indications of such phenomena in ***some*** subjects but not in others (Bagley, 1987); however, some of this effect is probably related to "drifts" in subject attention.

Can this phenomenon be modeled? Edman et al (1978) suggested a few possible sources, including a viscoelastic effect and changes in the force–velocity relation or activation level. Crowe et al. (1980), using four length "bins" to represent length-dependency, found that the basic behavior of enhancement could be simulated, but that the predicted delay was too fast (within 1 sec). Reasonable force enhancement can be also be obtained if *Eq. 5.18* is modified by having an empirical "enhancement" factor added to the right side (see also curve *E* in Figure 5.16a):

$$F_{att}(A,v_{ce}) = F_{act}(A) - F_y(A,v_{ce}) + F_{enh}(A,v_{ce}) \quad (5.21)$$

Sprigings (1986), assuming a linearized Hill model structure, computed the time constant B_h/K_{se} and showed that if this time constant could somehow increase after stretch, enhancement could be modelled. He suggested that K_{se} is attachment-dependent and thus, with fewer bridges attached, K_{se} would decrease (i.e. compliance would increase). However, my own evaluation suggests that the magnitude of the compliance change doesn't seen to be enough to cause responses on the order of seconds. It should be noted, however, that the slope of the lengthening *CE* force–velocity curve is very large during small lengthening velocities (e.g. Katz, 1939). With both B_h increasing and K_{se} decreasing, as would be predicted by modern Hill models, the time constant may indeed be on the order of seconds. Additionally, passive viscoelastic tissue exhibits inherent force relaxation that can be on the order of seconds and even minutes (e.g. Fung, 1970). Thus, the concept of this having, in part, a mechanical origin describable from within the Hill model framework cannot be eliminated. However, in my opinion other sources, and particularly the issue of series sarcomere inhomogeneity addressed in Chapter 3 (Morgan), seems more appealing. There it is proposed that this phenomenon is related to cross-bridge uniformity, and there being an inherent tendency toward instability for muscle fibers longer than the rest length. Another approach towards modeling this effect, based on the "charge-transfer" model for muscle, is presented in Chapter 2 (Hatze).

5.4.3 Subtle Stiffness Effects

1. Sensitivity of SE/Stiffness Identification to Testing Method. A discrepancy between results from "quick release" experiments and the isometric "calculation" method (e.g., Parmley et al., 1970) that simple Hill models cannot explain. We saw in Section 5.2.2 that if the stiffness for each individual cross-bridge is assumed linear and the population in homogeneous), then for isometric contraction the stiffness would be a linear function of force, and thus the force–extension curve would then have an ***exponential shape***, similar to that traditionally used for biological soft tissues (*Figure 5.7c-d, Eq. 5.8-5.10)*, only here for a different reason.

In all other cases, however, force is of course ***not*** statically related to activation. When activation is higher than force (as during shortening of the *CE*), the force–extension curve would be expected to be more flat; when lower (e.g. lengthening *CE*), a more concave relationship would be expected. Since different methods for estimating *SE* utilize different activation operating ranges, this may help explain different results for different tests. As we saw in Section 5.2.2, the Hill *SE* relation can be made directly activation-dependent. Finally, Hill (1970) has suggested that part of the discrepancy may be due to passive viscoelastic effects; this possibility is best explored from within the framework of the Hill model structure.

2. Stiffness Variation During Isometric Contraction. Gassar and Hill (1924) found muscle to be especially "rigid" right after the initiation of stimulation (leading muscle force). Cecchi et al. (1984) and Stein and Gordon (1986) have carefully quantified changes in stiffness during isometric contraction, showing that stiffness ***leads*** force during the rising phase of tetanic isometric contraction, as if it was in part a function of activation. However, stiffness ***lags*** behind force (and even more so activation) during relaxation; such results are not consistent with the concept of stiffness being a static function of force and activation, and thus this subtle effect is very difficult to incorporate within the Hill model structure [or certain forms of Huxley-based models (Bobet et al., 1990)].

3. Transient Force "Dip" During Fast Releases. Another "unusual" effect is the transient force response

to very, very fast releases of low magnitude (< 0.5%), where an excessive force "dip" occurs over the time course of a few milliseconds and then recovers to a plateau before drifting back (Huxley and Simmons, 1971). This behavior cannot be represented by a single series stiffness element, and has been used as evidence of a mechanically induced change in attachment states [see McMahon (1984) for review]. McMahon also suggests that it cannot be explained by a Kelvin model of Figure 5.5c (however, at such high speeds both viscous and muscle mass effects will be more prominent and may play a role). Of note is that this phenomenon has little relevance to the study of multiple muscle movement systems because of the smoothing effects of system inertia and tendon compliance (Alexander, 1988).

5.5 Comparison to Simpler Models.

Simpler muscle models include: ***i)*** an idealized force generator; ***ii)*** a force generator that produces a smoothed (filtered) version of the rectified *EMG*; ***iii)*** a spring; or ***iv)*** parallel arrangement of spring and dashpot. Each of these approaches is fundamentally flawed, yet each is used successfully within this book. These models tend to be flawed because muscle force depends not only on the neural input, as represented by an *EMG*, but also on muscle length and velocity. Muscle dynamic properties clearly cannot be captured by a spring, nor in most cases by a parallel arrangement of spring and dashpot. Winters and Stark (1987) have shown, however, that higher-order Hill-based models can, over limited operating ranges, take on the input-output characteristics of lower-order models. Predictably, however, the required describing parameters change dramatically with the type of task, and even during a task.

Nonetheless, simpler models can be quite useful (and even preferable) as long as the range of applicability is firmly established. Of note is that whenever an *EMG* trajectory is causally related to a motor task in implicit model has been assumed. Table 5.1 provides a few insights, based on modeling experiences of myself and simulation results presented by other contributors, that could be used as "rules of thumb" to aid interpretation of experimental data.

Table 5.1: "Rules of Thumb" regarding Muscle Dynamics for Various Tasks

TASK	*Parameter Sensitivity* CE_{Vmax}	SE_{Xmax}	*Comments*
Shortening muscles in general	+ +	+	Lower force relative to *EMG* (reaching about 25% at higher velocities
Moderate- and high-speed "point-to-point" movements.	+ +	+	Assuming bell-shaped velocity patterns: ***Agonist:*** shape of force trajectory differs from *EMG* shape, with force especially low during higher velocity region and often showing a second "hump" even if *EMG* doesn't (e.g. Figures 19.6-19.11). ***Antagonist:*** force potentially relatively high if not turned "off" in time – a reason for the common observation of the antagonist turning "off" just before the agonist turns "on". Very effective at generating "clamping" force (assuming yielding doesn't occur).
Voluntary "stretch-shortening" movements	+ + +	+ +	***Antagonist-becoming-agonist:*** *CE* length transition will lead that for the overall muscle as the muscle force goes into a favorable *CE* operating range and to some extent elastic energy is released; thus the muscle force will be relatively higher than the *EMG* trace might indicate (see Chapters 38-39). ***Agonist-becoming-antagonist:*** normally *EMG* will have subsided early enough such that the low level of *EMG* that is seen does in fact represent low muscle force levels.
Elastic Bounce (prepared impact)	+ +	+ + +	Pre-impact *EMG* helps set up elastic recoil potential and helps assure that *CE* and *SE* are within the effective operating range; the force and work done may be higher than might be predicted from the *EMG*s. Unlike the case for voluntary stretch-shorting, antagonist co-contraction, which increases impedance, may be utilized effectively.
Aggressive Manual Tracking	+ +	+ +	Nonlinear models are much more effective at tracking, especially when quick direction changes are desired. Expect pulse-like *EMG*s and variable cocontraction, features which can make the mechanical system "look different" at different times.
Movements under high bias loads (e.g. isotonic, torso during tasks)	+	+ +	Due to lower velocities, the forces during shortening movements can be much higher than during "free" movements with the same *EMG*s.
Postural/equilibrium	+	+ +	Often a static *EMG*-force relation is appropriate, but use caution – the *CE* force–velocity relation is quite steep near zero velocity, and hence even slow lengthening muscle may generate 20-30% more force than predicted from an isometric *EMG*-force calibration; the converse, though not as dramatic, holds for shortening muscle.
Manipulation Tasks/Interaction with Environment	+ +	+ +	Both sensory feedback and cocontraction will be used aggressively as necessary. For dynamic tasks, the *SE* plays a major role in this regard. Hard to generalize since manipulation tasks differ significantly and since the hand and upper limb (and torso) muscles will be used quite differently. *EMG* and muscle force may bear little resemblence to each other when the task is complex – modeling becomes necessary.

5.6 Future Directions

There is a great need for experiments in the ***sub-maximal*** activation region, which is of greatest importance for "normal" human movement. Most individuals go through their entire day without maximally contracting muscles. Questions remain regarding sub-maximal relations for *CE* tension-length, *CE* force–velocity, *SE*, yielding, force enhancement, etc. Perhaps an "unwritten law" could be "passed" making it illegal to study muscle mechanics for maximally contracting muscles? For example, for activation-dependent *SE* characterization, it is suggested that future experiments should consider applying quick releases to steady ***sub-maximal*** isometric contraction, following the early lead of Joyce and Rack (1969).

Our emphasis here has been on utilizing carefully controlled experiments to illuminate muscle structure and properties. In many cases experiments are purposely designed to isolate certain elements within the model or to dramatically show certain experimental "quirks." For the "systems biomechanist" studying multiple muscle systems, however, the bottom line is the use of the model for the realistic tasks of special interest. Hopefully, the model provides insights into internal behavior and makes predictions that can be tested experimentally. Of note is that a model is more than just the sum of its components. The real "beauty" lies in the fact that the various elements ***interact dynamically*** with each other. Often "intuition" will fail unless actual simulations are performed – hence part of their value. How do we get maximum use out of a model? By following up "core" simulations with aggressive use of advanced tools such as the systematic study of the ***sensitivity of model behavior to model parameters***. Of note is that the relative sensitivity of model behavior to various parameters within a model is a function of the task. Another very helpful approach is maximizing insight is to employ task-specific linearization of a nonlinear model, followed by re-simulation. This process can be easily automated (Seif-Naraghi and Winters, 1989).

One of the best ways to simplify a model for a given class of tasks is to ***start*** with more complex nonlinear Hill-based models, as recommended here, and then identify insensitive model parameters # elements described by these parameters can then be linearized or eliminated with more confidence.

Ironically, significantly more effort has gone into ***creating*** models than in ***utilizing*** models. In this regard, this book is an exception, and perhaps a statement of what the future holds.

References

Abbott, B.C. and Aubert, X.M. (1951) The force exerted by active striated muscle during and after change in length. *J. Physiol. Lond.* **117**:77-86.

Abbott, B.C. and Wilkie, D.R. (1973) The relationship between velocity of shortening and the tension-length curve of skeletal muscle, *J. Physiol.* **120**:214-222.

Agarwal, G.C. and Golltieb, G.L. (1977) Oscillation of the human ankle joint in response to applied sinusoidal torque on the foot. *J. Physiol.* **268**:151-176.

Aubert, X. (1956) *Le Couplage Energetique de la Ccontraction Musculaire*. Brussels, Editions Arscia.

Alexander, R. McN. (1983) *Animal Mechanics* (Second Edition). Blackwell Sci. Publ., Oxford.

Alexander, R. McN. and Bennet-Clark, H.C. (1977) Storage of elastic strain energy in muscle and other tissues. *Nature* **265**:114-117.

Audu, M.L. and Davy, D.T. (1985) The influence of muscle model complexity in musculoskeletal motion modeling. *J. Biomech. Engng.* **107**:147-157.

Bagley, A.M. (1987) Analysis of human response to slow isokinetic movement. M.S. Thesis, Arizona State University.

Bahler, A.S. (1967) The series elastic element of mammalian skeletal muscle. *Am. J. Physiol.* **213**:1560-1564.

Bach, T.M., Chapman, A.E. and Calvert, T.W. (1983) Mechanical resonance of the human body during voluntary oscillations about the ankle joint. *J. Biomech.* **16**: 85-90.

Bahler, A.S. (1968) Modeling of mammalian skeletal muscle. *IEEE Trans. Biomed. Engng.* **BME-13**:248-257.

Baildon, R.W.A. and Chapman, A.E. (1983) A new approach to the human muscle model. *J. Biomech.* **16**:803-809.

Bennett, M.B., Ker, R.F., Dimery, N.J. and Alexander, R. McN. (1986) Mechanical properties of various mammalian tendons. *J. Zool.* **209**:537.

Bigland, B. and Lippold, O.C.J. (1954) The relation between force, velcoity and integrated electrical activity in human muscles. *J. Physiol.* **1253**:214-224.

Bobet, Stein, R.B. and Oguztoreli, M.N. (1990) Mechanisms relating force and high-frequency stiffness in skeletal muscle. *J. Biomech.*, accepted.

Bouchaert, J.P., Capellen, L. and de Blende, J. (1930) *J. Physiol.* **69**:473.

Butler, D.L., Grood, E.S., Noyes, F.R. and Zernicke,

R.F. (1979) Biomechanics of ligaments and tendon. *Exer. Sport Sci. Rev.* **6**:125-185.

Cavagna, G.A., Komarek, L., Citterio, G. and Margaria, R. (1971) Power output of the previously stretch muscle. *Med. Sport (Biomech. II)* **6**:159-167.

Cecchi, G., Griffiths, P.J. and Taylor, S.R. (1984a) The kinetics of crossbridge attachment studies by high frequency stiffness measurements. In *Contractile Mechanisms in Muscle* (Pollack, G.H. and Sugi, H., eds.), Plenum Press, pp. 641-655, New York.

Cecchi, G., Lombardi, V. and Menchetti, G. (1984b) Development of force-velcoity relation and rise of isometric tetanic tension measure the time course of different processes. *Pflugers Arch.* **401**:396-405.

Chapman, A.E. (1985) The mechancial properties of human muscle. *Exer. Sci. Sport Rev.* **13**: 443-501.

Chapman, A.E. and Calvert, T.W. (1979) Estimations of active-state from EMG recordings of human muscular contraction. *Electromyogr. Clin. Neurophys.* **19**:199-222.

Close, R.I. (1972) Dynamic properties of mammalian skeletal muscles. *Physiol. Rev.* **52**:129-197.

Cook, G. and Stark, L. (1968) The human eye movement mechanism: experiments, modelling and model testing. *Arch. Ophthal.* **79**:428-436.

Cordo, P.J. and Rymer, W.Zev (1982) Contributions of motor-unit recruitment and rate modulation to compensation for muscle yielding, *J. Neurophys.* **47**:797-809.

Crowe, A., Van Atteveldt, H. an Groothedde, H. (1980) Simulation studies of contracting skeletal muscles during mechanical strech. *J. Biomech.* **13**:333-340.

Dern, R.J., Levine, J.M. and Blair, H.A. (1947) Forces exerted at different velocities in human arm movement. *Am. J. Physiol.* **151**:415-437.

Ebashi, S.M. and Endo, M. (1968) Calcium ion and muscle contraction. *Prog. Biophys. Mol. Biol.* **18**:123.

Edman, K.A.P., Mulieri, L.A. and Scubon-Mulieri, B. (1976) Non-hyperbolic force-velocity relationship in single muscle fibres, *Acta Physiol. Scand.* **98**:143-156.

Edman, K.A.P., Elzinga, G. and Noble, M.I.M. (1978) Enhancement of mechanical performance by stretch during tetanic contractions of vertebrate skeletal muscle fibres. *J. Physiol.* **280**:139-155.

Elliott, D.H. (1965) Structure and function of mammalian tendon. *Biol. Rev.* **40**:392-425.

Fenn, W.O. and Marsh, B.S. (1935) Muscular force at different wpeeds of shortening. *J. Physiol. (Lond.)* **85**:277-297.

Flitney, F.W. and Hirst, D.G. (1978) Crossbridge detachment and sarcomere "give" during stretch in active frog's muscle. *J. Physiol.* **276**:449-465.

Ford, L.E., Huxley, A.F., and Simmons, R.M. (1977) Tension responses to sudden length change in stimulated frog muscle fibers near slack length. *J. Physiol.* **269**:441-515.

Fuchs, F. (1977) Cooperative interactions between calcium-binding sites on glycerinated muscle fibers - the influence of corss-bridge attachment. *Biochim. Biophys. Acta* **462**: 314-322.

Fung, Y.C. (1967) Elasticity of soft tissues in simple elongation. *Am. J. Physiol.* **213**:1532-1544.

Fung, Y.C. (1970) Mathematical representation of the mechanical properties of the heart muscle. *J. Biomech.* **3**:381-404.

Fung, Y.C. (1981) *Biomechanics.* Springer-Verlag, New York.

Gasser, H.S. and Hill, A.V. (1924) The dynamics of muscle contraction. *Proc. Roy Soc.* **96**:398-437.

Gielen, C.C.A.M. and Houk, J.C. (1987) A model of the motor servo: incorporating nonlinear spindle receptor and muscle mechanical properties. *Biol. Cybern.* **57**:217-235.

Gordon, A.M., Huxley, A.F. and Julian, F.J. (1966) The variation in isometric tension with sarcomere length in vertebrate muscles. *J. Physiol.* **184**:170-192.

Goubel, F., Bouisset, S. and Lestinne, F. (1971) Determination of muscular compliance in the course of movement. *Med. Sport (Biomech. II)* **6**:154-158.

Greene, P.R. and McMahon, T.A. (1979) Reflex stiffness of man's antigravity muscles during kneebends while carrying extra weights. *J. Biomech.* **12**:881-895.

Hanson, J. and Huxley, H.E. (1955) The structural basis of contraction in stiated muscle. *Symp. Soc. Exp. Biol.* **9**: 228-264.

Hatze, H. (1974) A model of skeletal muscle suitable for optimal motion problems. In: Biomech. IV, pp. 417-422, S. Karger, Basel.

Hatze, H. (1977) A myocybernetic control model of skeletal muscle. *Biol. Cybern.* **25**:103-119.

Hatze, H. (1981) *Myocybernetic Control Models of Skeletal Muscles.* Univ. of South Africa.

Henneman, E., Somjen, G. and Carpenter, D. (1965) Excitability and inhibitability of motoneurons of different sizes. *J. Neurobiol.* **28**: 599-620.

Hill, A.V. (1922) The maximum work and mechanical efficiency of human muscles, and their most economical speed. *J. Physiol.* **56**:19-45.

Hill, A.V. (1938) The heat of shortening and the dynamic constants of muscle. *Proc. Roy. Soc.* **B126**:136-195.

Hill, A.V. (1949) The abrupt transition from rest to activity in muscle. *Proc. Roy. Soc.* **B126**:399-420.

Hill, A.V. (1950) The series elastic component of muscle. *Proc. Roy. Soc.* **B141**:104-117.

Hill, A.V. (1970) *First and last experiments in muscle mechanics.*, Cambridge Univ. Press, Cambridge.

Hof, A.L. and Van den Berg, J. (1981) EMG to force processing. I. An electrical analogue of the Hill

muscle model. *J. Biomech.* **14:**747-758.

Huxley, A.F. and Simmons, R.M. (1971) Proposed mechanism of force generation in striated muscle. *Nature* **233:**533-538.

Jewell, B.R. and Wilkie, D.R. (1958) An analysis of the mechanical components in frog striated muscle. *J. Physiol.* **143:**515-540.

Joyce, G.C and Rack, P.M.H. (1969) Isotonic lengthening and shortening movements of cat soleus muscle. *J. Physiol.* **204:**475-495.

Joyce, G.C., Rack, P.M.H. and Ross, H.F. (1974) The forces generated at the human elbow joint in response to imposed sinusoidal movements of the forearm. *J. Physiol.* **240:**375-396.

Joyce, G.C., Rack, P.M.H. and Westbury, D.R. (1969) The mechanical properties of cat soleus muscle during controlled lengthening and shortening movements, *J. Physiol.* **214:**461-474.

Julian, F.J. and Sollins, M.R. (1973) Regulation of force and speed of shortening in muscle contraction. *Cold Spring Harbor Symp. Quanrt. Biol.* **37:**635-646.

Katz, B. (1939) The relation between force and speed in muscular contraction. *J. Physiol.* **96:**45-64.

Kleweno, D.K. (1987) Physiological and theoretical analysis of isometric strength curves of the upper limb. M.S. Thesis, Arizona State University.

Kleweno, D.K. and Winters, J.M. (1988) Sensitivity of upper-extremity strength curves to 3-D geometry: model results, *Adv. in Bioengng.*, ASME-WAM, **BED-8:** 53-56.

Komi, P.V. (1973) Relationship between muscle tension, EMG and velocity of contraction under concentric and eccentric work. In *New Developments in Electromyography and Clinical Neurophysiology*, (Desmedt, J.E., ed.), S. Karger, Basel, pp. 596.

Kulig, K., Andrews, J.G. and Hay, J.G. (1984) Human strength curves. *Exerc. Sport Sci. Rev.* **12:** 81-121.

Levin, A. and Wyman, J. (1927) The viscous elastic porperties of muscle. *Proc. Roy. Soc.* **B101:**218-243.

Lehman, S.L. and Stark., L. (1979) Simulation of linear and nonlinear eye movement models: sensitivity analysis and enumeration studies of time optimal control. *J. Cybern. Inform. Sci.* **2:**21-43.

Lehman, S.L. and Stark, L. (1982) Three algorithms for interpreting models consisting of ordinary differential equations: sensitivity coefficients, sensitivity functions, global optimization. *Math. Biosci.* **62:**107-122.

Ma, S. and Zahalak, G.I. (1987) Activation dynamics for a distribution-momnet model of skeletal muscle. *Proc. 6th Int. Conf. Math. Model.* **11:**778-782., St. Louis.

McCrorey, H.L., Gale, .H. and Alpert, N.R. (1966) Mechanical properties of the cat tenuissimus muscle. *Am. J. Physiol.* **210:**114-120.

McMahon, T.A. (1984) *Muscles, Reflexes and Locomotion.* Princeton Univ. Press, Princeton.

Morgan, D.L. (1977) Separation of active and passive components of short-range stiffness of muscle. *Amer. J. Physiol.* **232:**C45-C49.

Otten, E. (1988) Concepts and models of functional architecture in skeletal muscle. *Exer. Sport Sci. Rev.* 89-137.

Parmley, W.W., Yeatman, L.A. and Sonnenblick, E.H. (1970) Differences between isotonic and isometric force-velocity relations in cardiac and skeletal muscle. *Am. J. Physiol.* **219:**546-550.

Partridge, L.D. (1979) Muscle properties: a problem for the motor controller physiologist. In *Posture and Movement* (Talbott, R.E. and Humphery, D.R., eds.), pp. 189-229, Raven Press, New York.

Perrine, J.J. and Edgerton, V.R. (1978) Muscle force-velocity and power-velocity relationships under isokinetic loading. *Med. Sci. Sports* **10:** 159-166.

Petrofsky, J.S. and Phillips, C.A. (1981) The influence of temperature, initital length and electrical ativity on the force-velocity relationship of the medidal gastrocnemius muscle of the cat. *J. Biomech.* **14:**297-306.

Pertuzon, E. and Bouisset, S. Instantaneous force-velocity relationship in human muscle. *Med. Sport, Biomech. III*, **8:** 230-234.

Proske, U. and Morgan, D.L. (1987) Tendon stiffness: methods of measurement and significance for the control of movement. A review. *J. Biomech.* **20:**75-82.

Rack, P.M.H. and Ross, H.F. (1984) The tendon of flexor pollicis longus: its effects on the muscular control of force and position at the thumb. *J. Physiol.* **351:** 99-110.

Rack, P.M.H. and Westbury, D.R. (1969) The effects of length and stimulus rate on tension in isometric cat soleus muscle. *J. Physiol.* **204:**443-460.

Rack, P.M.H. and Westbury, D.R. (1974) The short range stiffness of active mammalian muscle and its effect on mechanical properties. *J. Physiol.* **240:**331-350.

Rack, P.M. and Westbury, D.R. (1984) Elastic properties of the cat soleus tendon and their functional importance. *J. Physiol.* **347:**479.

Ralston, H.J., Polissart, M.J., Inman, V.T., Close, J.R. and Feinstein, B. (1949) Dynamic features of human isolated voluntary muscle in isometric and free contractions. *J. Appl. Physiol.* **1:**526-533.

Ramsey, R.W. and Street, S.F. (1940) The isometric length tension diagram of isolated skeletal muscle fibers of the frog. *J. Cell. Comp. Physiol.* **15:**11-34.

Seif-Naraghi, A.H. and Winters, J.M. (1989) Effect of task-specific linearization on musculoskeletal system control strategies. *ASME Biomech. Symp.*, **AMD-98:** 347-350.

Silver-Thorn, M.B. (1987) Muscle imbalance in osteoarthritis of the human knee. M.S. thesis, Arizona State University.

Silver-Thorn, M.B. and Winters, J.M. (1988) Muscle imbalance and osteoarthritis of the knee. *Adv. in Bioengng.* ASME Wint. Ann. Mtng., **BED-8:** 95-98.

Sprigings, E.J. (1986) Simulation of the force enhancement phenomenon in muscle. *Comput. Biol. Med.* **16:**423-430.

Stein, R.B. and Gordon, T. (1986) Nonlinear stiffness-force relationships in whole mammalian skeletal muscles. *Can. J. Physiol. Pharmacol.* **64:**1236-1244.

Sugi, H. (1979) The origin of the series elasticity in striated muscle fibers. In *Cross-Bridge Mechanism in Muscle Contraction* (Sugi, H. and Pollack, G.H., eds.), pp. 85-102, Univ. of Tokyo Press, Tokyo.

Van Atteveldt, H. and Crowe, A. (1980) Active tension changes in frog skeletal muscle during and after mechancial extension. *J. Biomech.* **13:**323-335.

Van Dijk, J.H.M. (1978) Simulation of human arm movements controlled by peripheral feedback. *Biol. Cybern.* **29:**175-186.

Wells, J.B. (1964) Comparison of mechanical properties between slow and fast mammalian muscles. *J. Physiol.* **178:**252-269.

Wilkie, D.R. (1950) The relation between force and velocity in human muscle. *J. Physiol.* **K110:**248-280.

Wilkie, D.R. (1956) The mechanical properties of muscle. *Br. Med. Bull.* **12:**177-182.

Winters, J.M. (1985) Generalized analysis and design of antagonistic muscle models: effect of nonlinear muscle-joint properties on the control of fundamental movements. Ph.D. Dissertation, Univ. of Calif., Berkeley.

Winters, J.M. (1988) Improvements within the A.V. Hill model structure: strengths and limitations. *Proc. IEEE Engng. Med. Biol.*, pp. 559-560, New Orleans.

Winters, J.M. (1989) A novel approach for modeling transient lengthening with a Hill-based muscle model. *XII Int. Congr. Biomech.*, Abstract 128., Los Angeles.

Winters, J.M. and Bagley, A.M. (1987) Biomechanical modelling of muscle-joint systems: why it is useful. *IEEE Engng. Med. Biol.* **6:** 17-21.

Winters, J.M. and Stark, L. (1985) nalysis of fundamental movement patterns through the use of in-depth antagonistic muscle models. *IEEE Trans. Biomed. Engng.* **BME-32:** 826-839.

Winters, J.M. and Stark, L. (1987) Muscle models: what is gained and what is lost by varying model complexity. *Biol. Cybern.* **55:** 403-420.

Winters, J.M. and Stark, L. (1988) Estimated mechanical properties of synergistic muscles involved in movements of a variety of human joints. *J. Biomech.* **21:** 1027-1042.

Winters, J.M., Stark, L. and Seif-Naraghi, A.H. (1988) An analysis of the sources of muscle-joint system impedance. *J. Biomech.* **21:** 1011-1026.

Woittiez, R.D., Huijing, P.A., Boom, H.B.K. and Rozendal, R.H. (1984) A three-dimensional muscle model: a quantified relation between form and function of skeletal muscles, *J. Morphol.* **182:**95-113.

Yates, J.W. and Kamon, E. (1983) A comparison of peak and constant angle torque-velcoity curves in fast and slow-twitch populations. *Eur. J. Appl. Physiol.* **51:**67-74.

Zahalak, G.I. (1981) A distribution-moment approximation for kinetic theories of muscular contraction. *Math. Biosci.* **55:** 89-114.

Zahalak, G.I., Duffy, J., Stewart, P.A., Litchman, H.M., Hawley, R.H. and Pasley, P.R. (1976) Partially activated human skeletal muscle: an experimental investigation of force, velocity and EMG. *J. Appl. Mech.* **98:** 81-86.

Zahalak, G.I. and Heyman, S.J. (1979) A quantitative evaluation of the frequency-response characteristics of active human skeletal muscle in vivo. *J. Biomech. Engng.* **28:** 28-37.

Zajac, F. (1989) Muscle and tendon: properties, models, scaling and application to biomechanics and motor control. *CRC Crit. Rev. Biomed. Engng.* **17:**359-415.